Copyright Warning & Restrictions

The copyright law of the United States (Title 17, United States Code) governs the making of photocopies or other reproductions of copyrighted material.

Under certain conditions specified in the law, libraries and archives are authorized to furnish a photocopy or other reproduction. One of these specified conditions is that the photocopy or reproduction is not to be "used for any purpose other than private study, scholarship, or research." If a, user makes a request for, or later uses, a photocopy or reproduction for purposes in excess of "fair use" that user may be liable for copyright infringement,

This institution reserves the right to refuse to accept a copying order if, in its judgment, fulfillment of the order would involve violation of copyright law.

Please Note: The author retains the copyright while the New Jersey Institute of Technology reserves the right to distribute this thesis or dissertation

Printing note: If you do not wish to print this page, then select "Pages from: first page # to: last page #" on the print dialog screen

ABSTRACT

SUBSPACE METHODS FOR PORTFOLIO DESIGN

by
Onur Yilmaz

Financial signal processing (FSP) is one of the emerging areas in the field of signal processing. It is comprised of mathematical finance and signal processing. Signal processing engineers consider speech, image, video, and price of a stock as signals of interest for the given application. The information that they will infer from raw data is different for each application. Financial engineers develop new solutions for financial problems using their knowledge base in signal processing. The goal of financial engineers is to process the harvested financial signal to get meaningful information for the purpose.

Designing investment portfolios have always been at the center of finance. An investment portfolio is comprised of financial instruments such as stocks, bonds, futures, options, and others. It is designed based on risk limits and return expectations of investors and managed by portfolio managers. Modern Portfolio Theory (MPT) offers a mathematical method for portfolio optimization. It defines the risk as the standard deviation of the portfolio return and provides closed-form solution for the risk optimization problem where asset allocations are derived from. The risk and the return of an investment are the two inseparable performance metrics. Therefore, risk normalized return, called Sharpe ratio, is the most widely used performance metric for financial investments.

Subspace methods have been one of the pillars of functional analysis and signal processing. They are used for portfolio design, regression analysis and noise filtering in finance applications. Each subspace has its unique characteristics that may serve requirements of a specific application. For still image and video compression applications, Discrete Cosine Transform (DCT) has been successfully employed in

transform coding where Karhunen-Loeve Transform (KLT) is the optimum block transform.

In this dissertation, a signal processing framework to design investment portfolios is proposed. Portfolio theory and subspace methods are investigated and jointly treated. First, KLT, also known as eigenanalysis or principal component analysis (PCA) of empirical correlation matrix for a random vector process that statistically represents asset returns in a basket of instruments, is investigated. Auto-regressive, order one, AR(1) discrete process is employed to approximate such an empirical correlation matrix. Eigenvector and eigenvalue kernels of AR(1) process are utilized for closed-form expressions of Sharpe ratios and market exposures of the resulting eigenportfolios. Their performances are evaluated and compared for various statistical scenarios. Then, a novel methodology to design subband/filterbank portfolios for a given empirical correlation matrix by using the theory of optimal filter banks is proposed. It is a natural extension of the celebrated eigenportfolios. Closed-form expressions for Sharpe ratios and market exposures of subband/filterbank portfolios are derived and compared with eigenportfolios.

A simple and powerful new method using the rate-distortion theory to sparse eigen-subspaces, called Sparse KLT (SKLT), is developed. The method utilizes varying size mid-tread (zero-zone) pdf-optimized (Lloyd-Max) quantizers created for each eigenvector (or for the entire eigenmatrix) of a given eigen-subspace to achieve the desired cardinality reduction. The sparsity performance comparisons demonstrate the superiority of the proposed SKLT method over the popular sparse representation algorithms reported in the literature.

SUBSPACE METHODS FOR PORTFOLIO DESIGN

by
Onur Yilmaz

A Dissertation
Submitted to the Faculty of
New Jersey Institute of Technology
in Partial Fulfillment of the Requirements for the Degree of
Doctor of Philosophy in Computer Engineering

Helen and John C. Hartmann Department of
Electrical and Computer Engineering

May 2016

APPROVAL PAGE

SUBSPACE METHODS FOR PORTFOLIO DESIGN

Onur Yilmaz

Dr. Ali N. Akansu, Dissertation Advisor — Date
Professor of Electrical and Computer Engineering, NJIT

Dr. Ali Abdi, Committee Member — Date
Associate Professor of Electrical and Computer Engineering, NJIT

Dr. Richard A. Haddad, Committee Member — Date
Professor Emeritus of Electrical and Computer Engineering, NJIT

Dr. Marvin K. Nakayama, Committee Member — Date
Professor of Computer Science, NJIT

Dr. Cheickna Sylla, Committee Member — Date
Professor of School of Management, NJIT

BIOGRAPHICAL SKETCH

Author: Onur Yilmaz

Degree: Doctor of Philosophy

Date: May 2016

Undergraduate and Graduate Education:

- Doctor of Philosophy in Computer Engineering,
  New Jersey Institute of Technology, Newark, NJ, 2016
- Master of Science in Computer Science,
  Ege University, Izmir, Turkey, 2011
- Bachelor of Science in Computer and Instructional Technologies Teaching,
  Ege University, Izmir, Turkey, 2007

Major: Computer Engineering

Presentations and Publications:

Mustafa U. Torun, Onur Yilmaz, and Ali N. Akansu, "FPGA, GPU, and CPU Implementations of Jacobi Algorithm for Eigenanalysis," *submitted to Journal of Parallel and Distributed Computing.*

Mustafa U. Torun, Onur Yilmaz, and Ali N. Akansu, "Explicit Kernel and Sparsity of Eigen Subspace for AR(1) Process," Book Chapter in *Financial Signal Processing and Machine Learning*, A. N. Akansu, S. R. Kulkarni and D. Malioutov, Eds., Hoboken, NJ, USA: Wiley-IEEE Press, 2016.

Onur Yilmaz, and Ali N. Akansu, "Performance Analysis of Eigenportfolios for AR(1) Process," *50th Annual Conference on Information Sciences and Systems (CISS)*, Princeton, NJ, 2016.

Onur Yilmaz, and Ali N. Akansu, "A Method to Sparse Eigen Subspace and Eigenportfolios," *18th International Conference on Information Fusion*, Washington, DC, 2015.

Onur Yilmaz, and Ali N. Akansu, "Quantization of Eigen Subspace for Sparse Representation," *IEEE Transactions on Signal Processing*, vol. 63, no. 14, pp. 3616-3625, 2015.

Onur Yilmaz, Mustafa U. Torun, and Ali N. Akansu, "A Fast Derivation of Karhunen-Loeve Transform Kernel for First-Order Autoregressive Discrete Process," *ACM SIGMETRICS Performance Evaluation Review*, vol. 41, no. 4, pp. 61-64, 2014.

Onur Yilmaz, Orhan Dagdeviren, and Kayhan Erciyes, "Localization free and Energy Efficient Hole Bypassing Techniques for Fault Tolerant Sensor Networks," *Journal of Network and Computer Applications*, vol. 40, pp. 164-178, 2014.

Mustafa U. Torun, Onur Yilmaz, and Ali N. Akansu, "FPGA Based Eigenfiltering for Real-Time Portfolio Risk Analysis," *IEEE International Conference on Acoustics, Speech and Signal Processing*, Vancouver, BC, 2013.

Mustafa U. Torun, Onur Yilmaz, and Ali N. Akansu, "Novel GPU Implementation of Jacobi Algorithm for Karhunen-Loeve Transform of Dense Matrices," *46th Annual Conference on Information Sciences and Systems (CISS)*, Princeton, NJ, 2012

Onur Yilmaz, Sercan Demirci, Yagiz Kaymak, Serkan Ergun, and Ahmet Yildirim, "Shortest Hop Multipath Algorithm for Wireless Sensor Networks," *Computers and Mathematics with Applications*, vol. 63, no. 1, pp. 48-59, 2012.

Onur Yilmaz, Orhan Dagdeviren, and Kayhan Erciyes, "Interference-Aware Dynamic Algorithms for Energy Efficient Topology Control in Wireless Ad Hoc and Sensor Networks," *The Computer Journal*, Oxford, 2011.

Kayhan Erciyes, Orhan Dagdeviren, Deniz Cokuslu, Onur Yilmaz, and Hasan Gumus, "Modeling and Simulation of Mobile Ad hoc Networks," Book Chapter in *Mobile ad hoc networks: Current status and Future trends*, J. Loo, J. L. Mauri, and J. H. Ortiz, Philadelphia, PA, USA: CRC Press, 2011.

Onur Yilmaz, and Kayhan Erciyes, "Distributed Weighted Node Shortest Path Routing Algorithm," *The Second International Conference on Wireless & Mobile Networks*, Ankara, Turkey, 2010.

Onur Yilmaz, and Sercan Demirci, Yagiz Kaymak and Kayhan Erciyes, "Synchronous Distributed Spanning Tree Algorithm for Wireless Sensor Networks," *1st International Symposium on Computing in Science & Engineering (ISCSE)*, Kusadasi, Turkey, 2010.

Sevgili annem, babam,
ve
canım eşim, Ece'ye

To my dear mom, dad,
and
my beloved wife, Ece

ACKNOWLEDGMENT

As a PhD student in New Jersey Institute of Technology (NJIT), I enjoyed the time I spent and the experiences I gained, despite the stressful and hard times. I learned how to be patient and strong, and how to overcome the difficulties no matter what the circumstances are. I deeply appreciate the support of many people because this dissertation would not have been possible without them.

First, I would like to thank my advisor, Prof. Ali N. Akansu, for his immense support, guidance, and patience during my doctoral study. He guided me through the treacherous paths of research. I will always be grateful to him for letting me study in his lab.

I am also grateful to Prof. Richard A. Haddad, and Prof. Ali Abdi of the ECE Department of NJIT; Prof. Marvin K. Nakayama of the CS Department of NJIT; and Prof. Cheickna Sylla of SOM of NJIT for serving on my dissertation committee and for their continued support.

I would like to thank NJIT for the financial support that made this study possible. I also appreciate the encouragement of Prof. Cüneyt Güzeliş to study at NJIT.

I always feel lucky to have companionship of Mustafa U. Torun, Yağız Kaymak, Kyle Marshall, Irfan Lateef, and Sina Fathi. I am thankful for their help and support.

The last and the most, I would like to thank my dear wife, Ece Yılmaz, for her priceless support and patience. Words fall short to express my feelings and gratitude to her. I would also like to thank my parents, Ali and Neşe Yılmaz, my parents-in-law, Murat and Nuran Güneyligil, and my sister-in-law, Cansu Güneyligil. If it were not for them, this work would not be possible.

TABLE OF CONTENTS

TABLE OF CONTENTS
(Continued)

Chapter **Page**

LIST OF TABLES

Table **Page**

LIST OF FIGURES

Figure **Page**

LIST OF FIGURES
(Continued)

Figure **Page**

LIST OF FIGURES
(Continued)

Figure **Page**

LIST OF FIGURES
(Continued)

Figure **Page**

CHAPTER 1

INTRODUCTION

Designing investment portfolios has always been at the center of the finance. The term, portfolio, refers to any collection of financial assets such as stocks, bonds, futures, options, and etc. Investment portfolios are managed by financial professionals, hedge funds, banks or other financial institutions and designed based on risk limits and return expectations of investors [2].

In a typical scenario, a portfolio manager creates a basket that is comprised of assets and designs capital allocation vector for the given risk limits and return expectations. Capital allocation vector includes the amount of money that will be invested to individual assets in the basket. Portfolio manager dynamically rebalances the allocations of the portfolio in order to minimize its risk for the targeted return performance. The risk and the return of an investment are the two inseparable performance metrics. Therefore, risk normalized return called Sharpe ratio is the most widely used performance metric for financial investments [2]

Modern Portfolio Theory (MPT), introduced by Markowitz, offers a mathematical method for portfolio optimization [32]. It models the return of an asset as normal (Gaussian) random variable and defines the investment risk as its standard deviation (volatility). Each asset in a portfolio has a weight, also called allocation coefficient, and the return of a portfolio is calculated as the weighted sum of asset returns. Portfolio volatility is shown to be a function of pairwise correlations among asset returns. MPT provides closed-form solution for the risk optimization problem. A portfolio with minimum risk for the targeted return is called efficient portfolio. Efficient frontier is generated by efficient portfolios on the risk-return plane [32].

Financial signal processing (FSP), is a relatively new area that is comprised of mathematical finance and signal processing. Signal processing engineers and financial professionals have been working on fundamentally similar problems for different applications. Financial engineers (signal processing engineers specialized to finance) offer possible improvements to the problems using the existing methods in signal processing[2].

Subspace methods have been the pillars of many applications in signal processing and finance. These applications exploit the signal properties in transform domain that is hidden in signal domain. Subspace is basically a surface in higher dimensional vector space. A given signal vector is projected onto the defined subspace and processed in the new domain.

Each subspace method has its unique characteristics that may serve the requirements of a specific application. The Fourier transform and its extensions have been the dominant transform for signal analysis and representation. For transform coding applications, Discrete Cosine Transform (DCT) has been employed successfully due its compression and decorrelation properties. The availability of fast implementation has made the DCT number of transform for image/video coding standards. Karhunen Loeve Transform (KLT), also known as principal component analysis (PCA) and eigenanalysis, is the optimal block transform with an orthonormal basis that maximizes the gain of transform coding (GTC) over pulse code modulation (PCM) and perfectly decorrelates the given signal in the subspace. Unlike DCT and Fourier transforms, KLT is signal dependent. Whenever the signal statistics is changed, its transform matrix has to be updated accordingly [1].

In block transforms (Fourier transform, DCT, KLT, etc.), the length of the basis functions is equal to the size of the input signal vector. Although this property brings many advantages such as easy and fast implementation, this structure limits

the possible freedom in tuning the basis functions in the time domain. Some of the requirements including orthogonality can be met.

If the length of these basis functions are extended in time, more freedom can be achieved to tune the basis functions for the desired properties. In general, if the arbitrary durations for these basis sequence filters is allowed, filter bank or subband concept is reached. Thus, block transforms can be considered as a special case of filter banks [1]. Due to arbitrary durations of basis sequences, the transform matrix is no longer square. Therefore it is not invertible. The subband (filter bank) theory provides mathematical requirements to design invertible subband subspaces (filter banks) [1].

In this dissertation, a unified treatment of subspace methods and MPT is proposed. Some of the subspace methods including KLT and subband transforms are investigated using the framework of MPT for finance applications. Auto-regressive order one, AR(1), process is utilized to model asset returns vector for all performance evaluations and comparisons. Closed-form expressions are derived for Sharpe ratio and market exposure of investment portfolios generated by the subspace methods. Moreover, the problem of generating sparse subspaces is investigated in this dissertation. Subspace sparsing framework, so called Sparse Karhunen Loeve Transform (SKLT), based on the rate-distortion theory is proposed. It is also shown that the proposed method outperform the popular algorithms in the literature.

Contributions of the dissertation include the following;

1. Unified treatment of subspace methods and MPT is proposed.
2. Eigenportfolios have been used in many investment strategies including statistical arbitrage. This dissertation analytically evaluates their performance with commonly used metrics such as Sharpe ratio and market exposure. Thus, it offers a better understanding of eigenportfolios behaviour for different scenarios.
3. Design of optimized super eigenportfolio (OSEP) is introduced. It is created by optimal allocation of investment capital among eigenportfolios based on maximization of Sharpe ratio.

4. Subband portfolios is introduced in this dissertation. Their performances are also evaluated and compared with eigenportfolios.

5. A new eigen subspace sparsing method, namely Sparse Karhunen Loeve Transform, based on the rate-distortion theory is proposed. Its performance is compared with the popular methods in the literature. It is shown that SKLT outperforms those methods for certain cases.

Further details on above points are given next. Outline of the dissertation is discussed at the end of the chapter.

1.1 Eigenportfolios

KLT is the optimal orthonormal subspace method (block transform) that maps wide-sense stationary (WSS) stochastic signals with correlations into non-stationary and pairwise uncorrelated transform coefficients [1]. It repacks the signal energy in a way that maximizes the GTC over PCM [1]. KLT basis functions are the eigenvectors of the given signal covariance matrix that define the corresponding unique eigen subspace.

N eigenportfolios with different risks and returns are created through the eigen decomposition of empirical correlation matrix of asset returns for a given N-asset basket. Each eigenvector is utilized as capital allocation vector. The returns of eigenportfolios are the coefficents of KLT.

Closed-form expressions for Sharpe ratios and market exposures of eigenportfolios are derived. Their performances for discrete AR(1) signal model and market data are calculated and compared. The proposed framework is extended to design optimized super eigenportfolio (OSEP) where investment capital is optimally allocated among multiple eigenportfolios based on maximization of Sharpe ratio. It is showed through a five-stock investment basket that AR(1) approximation closely mimics its empirical correlation matrix obtained from market data. The proposed framework presents new insights for eigenportfolios and trading algorithms like statistical arbitrage that utilize them.

1.2 Subband Portfolios

Subband decomposition is an another multiresolution signal decomposition method that has been widely used for data compression applications. In fact, block transforms such as KLT can be viewed as a special filter banks [1].

The objective is to extend the length of the basis functions in time to achieve freedom for tuning. Since the transform matrix is no longer square, it is not invertible. The subband (filter bank) theory provides mathematical framework to design invertible subband subspaces (filter banks) [1]

Optimal perfect reconstruction quadrature mirror filter (PR-QMF) that is proposed in [15, 14], is one of methods to design the perfect reconstruction filter banks. PR-QMF banks have been extensively used for splitting a signal into subbands in the frequency domain and each subband can be processed independently.

Optimal perfect reconstruction filter banks are utilized to generate M subband portfolios for a given N-asset basket where $M < N$. Closed-form expressions for Sharpe ratios and market exposures of subband portfolios are also analyzed and compared with eigenportfolios for discrete AR(1) signal model.

1.3 Quantization of Subspaces for Sparse Representations

KLT has been employed in multivariate data processing and dimension reduction, although the application specific interpretation of principal components (eigenvectors) is often difficult in some cases [13, 42, 49, 20]. Moreover, small but non-zero loadings (elements) of each principal component (PC) (or eigenvector) bring implementation cost that is hard to justify in applications such as generation and maintenance (rebalancing) of eigenportfolios in finance [20, 41, 2]. This and other applications that utilize loading coefficients have motivated researchers to study sparsity of PCs in eigen analysis of matrices.

The constrained optimization algorithms to generate sparse PCs are unable to guarantee good performance for an arbitrary covariance matrix due to the non-convex nature of the problem. A procedure to sparse subspaces is proposed in this dissertation. The proposed SKLT method utilizes the mathematical framework developed in rate-distortion theory for transform coding using pdf-optimized quantizers. The sparsity (cardinality reduction) is achieved through the pdf-optimized quantization of basis function (vector) set. It may be considered an extension of the simple and soft thresholding (ST) methods.

The merit of the proposed framework for sparse representation is presented for AR(1) signal model and empirical correlation matrix of stock returns for NASDAQ-100 index. The sparsity performance comparisons demonstrate the superiority of SKLT over the popular algorithms in the literature. SKLT is theoretically tractable, simple to implement and serves to sparse any subspace of interest.

1.4 Dissertation Outline

This dissertation is organized as follows. In Chapter 2, mathematical preliminaries required for the discussions in the later chapters are given. Topics discussed in this chapter include orthogonal transforms, discrete AR(1) signal model, eigenanalysis, closed-form kernel for the discrete AR(1) process, and transform coding.

In Chapter 3, Modern Portfolio Theory (MPT) is summarized. How to calculate normalized asset returns, portfolio risk and return are included in this chapter. Portfolio optimization of MPT and Markowitz Bullet are also discussed.

Eigenportfolios are introduced in Chapter 4. The performance analysis of eigenportfolios are included in this chapter. Sharpe ratio and market exposure of eigenportfolios for different discrete AR(1) model parameters are displayed and discussed. Moreover, the model is validated with real-market data.

Chapter 5 presents the concept of subband portfolios. Similar to Chapter 4, performance of subband portfolios are evaluated and compared with eigenportfolios. Their advantages and disadvantages are stressed in this chapter.

A method, called Sparse Karhunen Loeve Transform (KLT) to sparse eigen subspace is proposed in Chapter 6. The mathematical framework developed in rate-distortion theory for transform coding using pdf-optimized quantizers is utilized in this chapter. The merit of the proposed framework is evaluated and compared for AR(1) signal model and empirical correlation matrix of stock returns for NASDAQ-100 index. Discussions, concluding remarks, and future research plans are in Chapter 7.

CHAPTER 2

MATHEMATICAL PRELIMINARIES

Preliminary mathematical background for the discussions in the dissertation is given in this chapter. This chapter includes discrete auto-regressive one, AR(1), signal model, block transforms, gain of transform coding (GTC), eigendecomposition, closed-form kernel of KLT for AR(1) signal model and transform coding.

2.1 Discrete AR(1) Signal Model

Autoregressive discrete process of order one, AR(1), is a widely used model in the literature for performance analysis and comparison of signal processing methods. It is the first approximation of many signals like images and price of an asset. AR(1) process is expressed as [1]

$$x(n) = \rho x(n-1) + \xi(n) + c \tag{2.1}$$

where $\xi(n)$ is white noise sequence with zero-mean and variance σ_ξ^2, $E\{\xi(n)\xi(n+k)\} = \sigma_\xi^2 \delta_{n-k}$, and c is a constant. The first order correlation coefficient ρ of AR(1) model with $-1 < \rho < 1$ for wide-sense stationary process (WSS) is defined as

$$\begin{aligned} \rho &= R_{xx}(1) / R_{xx}(0) \\ &= \frac{E\{x(n)\, x(n+1)\}}{E\{x(n)\, x(n)\}} \end{aligned} \tag{2.2}$$

The mean of $x(n)$ is calculated as

$$\mu_x = E\{x(n)\} = \frac{c}{(1-\rho)} \tag{2.3}$$

And, its variance is found as

$$\sigma_x^2 = E\left\{x\left(n\right)^2\right\} - \mu_x^2 = \frac{\sigma_\xi^2}{(1-\rho^2)} \tag{2.4}$$

The autocorrelation sequence for AR(1) process is expressed as

$$R_{xx}(k) = E\left\{x(n)x(n+k)\right\} = \sigma_x^2 \rho^{|k|};\ k = 0, \pm 1, \pm 2, \ldots \tag{2.5}$$

The resulting Toeplitz correlation matrix of size $N \times N$ is shown to be in the form

$$\mathbf{R}_x = \sigma_x^2 \begin{bmatrix} 1 & \rho & \rho^2 & \cdots & \rho^{N-1} \\ \rho & 1 & \rho & \cdots & \rho^{N-2} \\ \rho^2 & \rho & 1 & \cdots & \rho^{N-3} \\ \vdots & \vdots & \vdots & \ddots & \vdots \\ \rho^{N-1} & \rho^{N-2} & \rho^{N-3} & \cdots & 1 \end{bmatrix} \tag{2.6}$$

AR(1) is a special WSS Gaussian process for $-1 < \rho < 1$. It has multivariate normal distribution $\mathbf{x} \sim N(\boldsymbol{\mu}, \mathbf{R}_x)$ for finite dimensions where

$$\begin{aligned} \boldsymbol{\mu} &= [\mu_k]\,; k = 1, 2, \ldots, N \\ \mu_k &= \mu_x \end{aligned} \tag{2.7}$$

2.2 Block Transforms

A discrete orthonormal transform (subspace) is described by a set of linearly independent N sequences (vectors), $\{\phi_k(n)\}$ $0 \leq n \leq N-1$, satisfying the inner product properties [1]

$$\sum_{n=0}^{N-1} \phi_k(n)\phi_l^*(n) = \delta_{k-l} = \begin{cases} 1, k = l \\ 0, otherwise \end{cases} \tag{2.8}$$

where n is the index of random variables in the vector process (or discrete-time). In matrix form, vectors (or basis sequences) $\boldsymbol{\phi}_k = \{\phi_k(n)\}$ are structured as the rows of the transform matrix

$$\Phi = [\phi_k(n)] : k, n = 0, 1, ..., N-1 \tag{2.9}$$

with the subspace orthonormality stated as

$$\Phi\Phi^{-1} = \Phi\Phi^{*\mathbf{T}} = \mathbf{I} \tag{2.10}$$

where $*\mathrm{T}$ indicates the conjugated and transposed version of a matrix, and $\mathbf{I}$ is the $N \times N$ identity matrix. The projection (forward transform) of and arbitrary vector $\mathbf{x}$ onto subspace is defined as

$$\boldsymbol{\theta} = \Phi\mathbf{x} \tag{2.11}$$

where $\boldsymbol{\theta}$ is the representation (transform) coefficient vector. Similarly, the representation (inverse transform) of $\mathbf{x}$ in the orthogonal subspace is expressed as

$$\mathbf{x} = \Phi^{-1}\boldsymbol{\theta} = \Phi^{*\mathrm{T}}\boldsymbol{\theta} \tag{2.12}$$

2.3 Eigendecomposition of Correlation Matrix

An eigenvalue λ and its paired eigenvector $\boldsymbol{\phi}$ of an $N \times N$ correlation matrix $\mathbf{R}_x$ satisfy the matrix equation [1]

$$\begin{aligned} \mathbf{R}_x\boldsymbol{\phi} &= \lambda\boldsymbol{\phi} \\ \mathbf{R}_x\boldsymbol{\phi} - \lambda\mathbf{I}\boldsymbol{\phi} &= (\mathbf{R}_x - \lambda\mathbf{I})\,\boldsymbol{\phi} = 0 \end{aligned} \tag{2.13}$$

such that $(\mathbf{R}_x - \lambda\mathbf{I})$ is singular. Namely,

$$\det(\mathbf{R}_x - \lambda\mathbf{I}) = 0 \tag{2.14}$$

$\mathbf{R}_x$ of AR(1) process, described next in (2.6), is a real and symmetric matrix, and its eigenvectors are linearly independent. Thus, this determinant is a polynomial in λ of degree N, (2.14) has N roots and (2.13) has N solutions for $\boldsymbol{\phi}$ that result in eigenpair set $\{\lambda_k, \boldsymbol{\phi}_k\}\,;\, 0 \leq k \leq N-1$. Therefore, the eigendecomposition of $\mathbf{R}_x$ is expressed as [1]

$$\mathbf{R}_x = \mathbf{A}_{\mathbf{KLT}}^{\mathbf{T}} \boldsymbol{\Lambda} \mathbf{A}_{\mathbf{KLT}} = \sum_{k=0}^{N-1} \lambda_k \boldsymbol{\phi}_k \boldsymbol{\phi}_k^{\mathrm{T}} \tag{2.15}$$

where $\boldsymbol{\Lambda} = diag\,(\lambda_k)\,;\; k = 0, 1, \ldots, N-1$, and k^{th} *column* of $\mathbf{A}_{\mathbf{KLT}}^{\mathbf{T}}$ matrix is the k^{th} eigenvector $\boldsymbol{\phi}_k$ of $\mathbf{R}_x$ with the corresponding eigenvalue λ_k. Note that

$$\left\{\lambda_k = \sigma_k^2 = \boldsymbol{\phi}_k^{\mathrm{T}} \mathbf{R}_x \boldsymbol{\phi}_k\right\} \forall k \tag{2.16}$$

for the given $\mathbf{R}_x$ where σ_k^2 is the variance of the k^{th} transform coefficient, θ_k.

Note that $\{\lambda_k\}$ are sorted in descending order after the eigenvalues and eigenvectors are calculated. Therefore, first principal component (PC1) is placed in the first column of $\mathbf{A}_{KLT}$ matrix where $k = 0$.

2.4 Closed-form Expressions for Eigenvectors and Eigenvalues of AR(1) Process

The eigenvalues of $\mathbf{R}_x$ for an AR(1) process defined in (2.6) are expressed in the closed-form as [40, 36]

$$\sigma_k^2 = \lambda_k = \frac{1-\rho^2}{1 - 2\rho\cos(\omega_k) + \rho^2}; 0 \leq k \leq N-1 \tag{2.17}$$

where $\{\omega_k\}$ are the positive roots of the transcendental equation

$$\tan(N\omega) = -\frac{(1-\rho^2)\sin(\omega)}{\cos(\omega) - 2\rho + \rho^2\cos(\omega)} \tag{2.18}$$

that is rewritten as

$$\begin{aligned} &\left[\tan\left(\omega\frac{N}{2}\right) + \gamma\tan\left(\frac{\omega}{2}\right)\right]\left[\tan\left(\omega\frac{N}{2}\right) - \frac{1}{\gamma}\cot\left(\frac{\omega}{2}\right)\right] = 0 \\ &\gamma = (1+\rho)\,/\,(1-\rho)\,, \end{aligned} \tag{2.19}$$

The resulting KLT kernel for matrix of size $N \times N$ is expressed as [40, 36]

$$\begin{aligned} &\mathbf{A}_{KLT} = [A(k,n)] = c_k \sin\left[\omega_k\left(n - \frac{N-1}{2}\right) + \frac{(k+1)\pi}{2}\right] \\ &c_k = \left(\frac{2}{N+\lambda_k}\right)^{1/2},\ 0 \le k, n \le N-1 \end{aligned} \tag{2.20}$$

The roots of the transcendental tangent equation in (2.19), $\{\omega_k\}$, are required in the KLT kernel expressed in (2.20). An efficient root finding method for explicit solutions of transcendental equations including (2.19) was proposed in [40]. That method leads to an explicit KLT matrix kernel for an AR(1) process as given in (2.20).

2.5 Transform Coding

Historically speaking, transform coding (TC) of image and video signals has been one of the most popular applications of subspace methods where the desired dimension reduction is achieved through quantization of transform coefficients [1, 26, 17]. Original forward and inverse transform matrices are utilized in such a scenario. Quantization of coefficients in the transform domain, called transform coding (TC), is defined as

$$\widehat{\boldsymbol{\theta}} = Q\left\{\boldsymbol{\theta}\right\} \tag{2.21}$$

Then, reconstructed signal with quantized coefficient vector $\widehat{\boldsymbol{\theta}}$ is expressed as

$$\widehat{\mathbf{x}} = \Phi^{*\mathrm{T}}\widehat{\boldsymbol{\theta}} \tag{2.22}$$

The mean square error between the original and reconstructed signal due to quantization of coefficients is written as [1]

$$\sigma^2_{\epsilon,TC} = \frac{1}{N}E\left\{\widetilde{\mathbf{x}}^{\mathbf{T}}\widetilde{\mathbf{x}}\right\} \tag{2.23}$$

for zero mean signal $\mathbf{x}$ where the quantization error $\widetilde{\mathbf{x}} = \mathbf{x} - \widehat{\mathbf{x}}$. Similarly, the mean square error between the original and quantized coefficients in the transform domain is calculated as

$$\sigma^2_{q,TC} = \frac{1}{N}E\left\{\widetilde{\boldsymbol{\theta}}^{\mathbf{T}}\widetilde{\boldsymbol{\theta}}\right\} = \frac{1}{N}\sum_{k=0}^{N-1}\sigma^2_{q_k,TC} \tag{2.24}$$

where $\widetilde{\boldsymbol{\theta}} = \boldsymbol{\theta} - \widehat{\boldsymbol{\theta}}$, and $\sigma^2_{q_k,TC} = E\left\{\left|\widetilde{\boldsymbol{\theta}}_k\right|^2\right\}$ is the variance of the quantization error for the k^{th} coefficient. Hence, $\sigma^2_{\epsilon,TC} = \sigma^2_{q,TC}$ for an orthonormal transform (subspace) [1].

Transform coding (TC) aims to achieve dimension reduction by repacking signal energy unevenly among the minimum possible transform coefficients. The transform coefficients of a signal are quantized for lossy compression (entropy reduction) where most become negligible and replaced by zero in a typical scenario. The benefit of TC over pulse code modulation (PCM) depends on the covariance properties of a given random vector process and has been studied in the literature [1, 26, 17, 6, 23].

Lloyd-Max [33, 29] quantizer is designed based on the mean square error (mse) criterion for a given probability density function (pdf). In TC, it defines optimal quantizer intervals (bins) and their bin representation (quanta) values according to the pdf of the k^{th} transform coefficient $\boldsymbol{\theta}_k$ in order to minimize $\sigma^2_{q_k,TC}$ with the constraint $\sigma^2_{q_k} = \sigma^2_{q_l}\ \forall k, l$. This quantization process is repeated for all transform coefficients [1].

pdf-Optimized Midtread Quantizer Quantizers (Q) may be categorized as midrise and midtread [26]. Midtread quantizer is preferred for applications requiring entropy reduction and noise filtering (or sparsity) simultaneously [23]. In this paper, we utilize a midtread quantizer type to quantize each basis function (components of each vector) of a transform to achieve sparse representation.

A celebrated design method to calculate optimum intervals (bins) and representation (quanta) values of a quantizer for the given input signal pdf, so called pdf-optimized quantizer, was independently proposed by Max and Lloyd [33, 29]. It assumes a random information source X with zero-mean and a known pdf function $p(x)$. Then, it minimizes quantization error in the mse sense and also makes sure that all bins of a quantizer have the same level of representation error. The quantization error of an L-bin pdf-optimized quantizer is expressed as follows

$$\sigma_q^2 = \sum_{k=1}^{L} \int_{x_k}^{x_{k+1}} (x - y_k)^2 \, p(x) dx \tag{2.25}$$

where quantizer bin intervals, $[x_k, x_{k+1}]$, and quanta values, y_k, are calculated iteratively. The necessary conditions for an mse based pdf-optimized quantizer are given as [33, 29]

$$\frac{\partial \sigma_q^2}{\partial x_k} = 0;\ k = 2, 3, \ldots, L$$
$$\frac{\partial \sigma_q^2}{\partial y_k} = 0;\ k = 1, 2, 3, \ldots, L \tag{2.26}$$

leading to the optimal unequal intervals and resulting quanta values as

$$x_{k,opt} = \frac{1}{2}\left(y_{k,opt} + y_{k-1,opt}\right);\ k = 2, 3, \ldots, L \tag{2.27}$$
$$y_{k,opt} = \frac{\int_{x_k}^{x_{k+1,opt}} xp(x)dx}{\int_{x_k}^{x_{k+1,opt}} p(x)dx};\ k = 1, 2, \ldots, L \tag{2.28}$$

where $x_{1,opt} = -\infty$ and $x_{L+1,opt} = \infty$. Sufficient condition to avoid local optimum in (2.26) is the log-concavity of the pdf function $p(x)$. Log-concave property holds for Uniform, Gaussian and Laplacian pdf types [26]. The representation point (quantum) of a bin in such a quantizer is its centroid that minimizes the quantization noise for the interval. The focus is in pdf-optimized quantizers with adjustable zero-zone, odd L or midtread quantizer, to sparse (quantize) the given input.

The discrepancy between input and output of a quantizer is measured by the signal-to-quantization-noise ratio (SQNR) [6]

$$SQNR(dB) = 10\log_{10}\left(\frac{\sigma_x^2}{\sigma_q^2}\right) \tag{2.29}$$

where σ_x^2 is the variance of an input with zero-mean and known pdf type, and expressed as

$$\sigma_x^2 = \int_{-\infty}^{\infty} x^2 p(x)dx \tag{2.30}$$

The first order entropy (rate) of the output for an L-level quantizer with such an input is calculated as [6, 12]

$$H = -\sum_{k=1}^{L} P_k \log_2 P_k \tag{2.31}$$
$$P_k = \int_{x_k}^{x_{k+1}} p(x)dx.$$

Optimum Bit Allocation Among Transform Coefficients In TC, the method to allocate the allowable total bit rate R among multiple transform coefficients (information sources) performs an important task. Transform coefficient variances σ_k^2 (or eigenvalues λ_k in KLT) are desired to be maximally uneven in order to achieve dimension reduction in TC. Hence, optimum bit allocation algorithm assigns bit rate R_k for quantization of coefficient θ_k in a way that makes the quantization error for each coefficient to be equal $\left(\sigma_{q_0}^2 = \sigma_{q_1}^2 = \ldots = \sigma_{q_{N-1}}^2\right)$ [1]. Then, the number of levels for the k^{th} quantizer, for coefficient θ_k, is found as

$$L_k = 2^{R_k} \tag{2.32}$$

Rate-distortion theory states that, the quantization error variance is expressed as [6]

$$\sigma_{q_k}^2 = f\left(R_k\right)\sigma_k^2 \tag{2.33}$$

where $f\left(R_k\right) = \gamma_k 2^{-2R_k}$ and σ_k^2 are the quantizer distortion function for a unit variance input and variance of the k^{th} coefficient, respectively. γ_k depends on the pdf type of information source θ_k and also called *fudge factor*. It is shown with the assumption that all coefficients have the same pdf type, optimum bit rates R_k allocated among multiple information sources for the given total bit budget of R are calculated as [1]

$$R_k = R + \frac{1}{2}\log_2 \frac{\sigma_k^2}{\left(\prod_{i=0}^{N-1}\sigma_i^2\right)^{\frac{1}{N}}} \tag{2.34}$$

where $R = \sum_{k=0}^{N-1} R_k$. Optimum bit allocation for the coefficient θ_k may yield a negative real number R_k. It implies that representing $\boldsymbol{\theta}_k$ even by zero causes a quantization error less than constrained coefficient distortion $\sigma_k^2 = \sigma_l^2$. Hence, a reduction of one dimension is achieved in the quantized signal representation. Note that $L_k = 2^{R_k}$ needs to be a positive integer number. Therefore, optimum bit allocation is an iterative process in its implementation.

2.6 Gain of Transform Coding

The gain of transform coding over pulse code modulation (PCM) of $N \times N$ unitary transform for a given input correlation is widely utilized in transform theory and defined as

$$G_{TC}^N = \frac{\frac{1}{N}\sum_{k=0}^{N-1}\sigma_k^2}{\left(\prod_{k=0}^{N-1}\sigma_k^2\right)^{\frac{1}{N}}} \tag{2.35}$$

where σ_k^2 is the variance of kth transform coefficient and N is the transform size.

2.7 Chapter Summary

Discrete AR(1) signal model has been widely used in signal processing and finance for performance comparisons. Closed-form expressions for its mean, variance and auto-correlation matrix are given in this chapter. Discrete AR(1) model forms the foundations of modeling and theoretical performance comparisons in this dissertation. Block transforms and basic operations such as forward and inverse transforms are also discussed. Eigendecomposition of a given correlation matrix which is the most

important step to generate eigenportfolios and closed-form expressions of eigenmatrix and eigenvalues for AR(1) model are summarized in this chapter. They will be utilized in Chapter 4 and Chapter 6. pdf-optimized midtread quantizer and optimum bit allocation algorithm that will be used in Chapter 6 to sparse a given subspace are also discussed. Lastly, gain of transform coding is revisited. It will be used in Chapter 5 to design subband portfolios.

CHAPTER 3

MODERN PORTFOLIO THEORY

In this chapter, celebrated Modern Portfolio Theory (MPT) is revisited in order to build the background of discussions about subspace methods and investment portfolios. It offers a framework to create risk minimized portfolio for a given expected return. Before the details of optimization problem, return and risk of a portfolio are defined.

3.1 Asset Returns

The normalized return of the kth asset of an N-asset portfolio is defined as [2, 41]

$$r_k(n) = \frac{p_k(n)}{p_k(n-1)} - 1;\ k = 1, 2, \ldots, N \tag{3.1}$$

where $p_k(n)$ is its price in discrete time n. Although histograms of asset returns for market data show fat-tails, excessive kurtosis and asymmetry properties, MPT assumes that the returns follow a normal distribution. The normality assumption makes statistical modeling and analysis tractable.

The mean and variance of $r_k(n)$ are calculated with the ergodicity assumption for a measurement window of W samples

$$\mu_k = E\{r_k(n)\} = \frac{1}{W}\sum_{m=0}^{W-1} r_k(n-m) \tag{3.2}$$

$$\sigma_k^2 = E\left\{r_k^2(n)\right\} - \mu_k^2 = \left[\frac{1}{W}\sum_{m=0}^{W-1} r_k^2(n-m)\right] - \mu_k^2 \tag{3.3}$$

where σ_k is the volatility of the kth asset.

3.2 Portfolio Return and Risk

The return vector of portfolio assets is defined as

$$\mathbf{r}(n) = [r_k(n)]\,; k = 1, 2, \ldots, N \tag{3.4}$$

The sampling time index n is omitted for convenience in the following discussions. Return of an N-asset portfolio is expressed as

$$r_p = \mathbf{q}^{\mathrm{T}}\mathbf{r} \tag{3.5}$$

where $\mathbf{q} = [q_k]\,; k = 1, 2, \ldots, N$ is the investment allocation vector. Portfolio risk (volatility) is defined as the standard deviation of portfolio return as follows [41]

$$\sigma_p = \left(E\left\{r_p^2\right\} - \mu_p^2\right)^{1/2} = \left(\mathbf{q}^{\mathrm{T}}\mathbf{C}\mathbf{q}\right)^{1/2} = \left(\mathbf{q}^{\mathrm{T}}\mathbf{\Sigma}^{\mathrm{T}}\mathbf{R}\mathbf{\Sigma}\mathbf{q}\right)^{1/2} \tag{3.6}$$

where

$$\mu_p = E\left\{r_p\right\} = \mathbf{q}^{\mathrm{T}}E\left\{\mathbf{r}\right\} = \mathbf{q}^{\mathrm{T}}\boldsymbol{\mu} \tag{3.7}$$

is the expected return of the portfolio, $\boldsymbol{\mu}$ is an $N \times 1$ vector populated with expected returns of assets, $\mathbf{\Sigma}$ is an $N \times N$ diagonal matrix with its elements $\{\sigma_k\}$ as standard deviations (volatilities) of asset returns, $\mathbf{C}$ is $N \times N$ covariance matrix of asset returns, and $\mathbf{R}$ is $N \times N$ correlation matrix where $[P_{ij}] = \rho_{ij}$. Correlation and covariance matrices are defined as

$$\mathbf{C} = [C(k,l)] = cov\left[r_k, r_l\right] = E\left\{r_k r_l\right\} - \mu_k\mu_l \tag{3.8}$$

$$\mathbf{R} = [R(k,l)] = \frac{cov\left[r_k, r_l\right]}{\sigma_k\sigma_l} = \frac{E\left\{r_k r_l\right\} - \mu_k\mu_l}{\sigma_k\sigma_l} \tag{3.9}$$

The covariance matrix is estimated with the ergodicity assumption for a measurement window of W samples as follows;

$$C(k,l) = \frac{1}{W} \sum_{m=0}^{W-1} r_k(n-m) r_l(n-m) \tag{3.10}$$

3.3 Sharpe Ratio and Market Exposure of Portfolio

Sharpe ratio of a portfolio is calculated as follows

$$S = \frac{\mu_p}{\sigma_p} \tag{3.11}$$

Sharpe ratio is the risk normalized return and it is an important metric in finance.

Market exposure is another important metric used in finance. It is the amount of investment with market risk (unhedged against market trend) and defined as

$$M_p = \sum_{i=1}^{N} \mathbf{q}_i \tag{3.12}$$

Note that this metric assumes that all asset returns in a basket have the same cross-correlation (co-movement) with the market return and perfect correlation among each other.

3.4 Portfolio Optimization

MPT provides a mathematical framework to create efficient portfolios from a basket of instruments with minimum risk for the targeted portfolio return [32]. The portfolio optimization problem in MPT is written as

$$\begin{aligned} \min \quad & \mathbf{q}^{\mathrm{T}}\mathbf{C}\mathbf{q} \\ \mathbf{s.t.} \quad & \mathbf{q}^{\mathrm{T}}\boldsymbol{\mu} = \mu \\ & \mathbf{q}^{\mathrm{T}}\mathbf{1} = 1 \end{aligned} \tag{3.13}$$

where μ is the targeted (expected) portfolio return. The closed-form solution for the optimization problem in (3.13) is given as

$$\mathbf{q} = \frac{\begin{vmatrix} \mu & \mathbf{1}^{\mathrm{T}}\mathbf{C}^{-\mathbf{1}}\boldsymbol{\mu} \\ 1 & \mathbf{1}^{\mathrm{T}}\mathbf{C}^{-\mathbf{1}}\mathbf{1} \end{vmatrix} \mathbf{C}^{-\mathbf{1}}\boldsymbol{\mu} + \begin{vmatrix} \boldsymbol{\mu}^{\mathrm{T}}\mathbf{C}^{-\mathbf{1}}\boldsymbol{\mu} & \mu \\ \boldsymbol{\mu}^{\mathrm{T}}\mathbf{C}^{-\mathbf{1}}\mathbf{1} & 1 \end{vmatrix} \mathbf{C}^{-\mathbf{1}}\mathbf{1}}{\begin{vmatrix} \boldsymbol{\mu}^{\mathrm{T}}\mathbf{C}^{-\mathbf{1}}\boldsymbol{\mu} & \mathbf{1}^{\mathrm{T}}\mathbf{C}^{-\mathbf{1}}\boldsymbol{\mu} \\ \boldsymbol{\mu}^{\mathrm{T}}\mathbf{C}^{-\mathbf{1}}\mathbf{1} & \mathbf{1}^{\mathrm{T}}\mathbf{C}^{-\mathbf{1}}\mathbf{1} \end{vmatrix}} \tag{3.14}$$

where $|.|$ is the matrix determinant operator, and $\mathbf{C}^{-\mathbf{1}}$ is the inverse of positive-definite $\mathbf{C}$ matrix. $\mathbf{1}$ is the $N \times 1$ unit vector where $\mathbf{1}^{\mathbf{T}} = \begin{bmatrix} 1 & 1 & \cdots & 1 \end{bmatrix}$. The set of optimum portfolios for the desired returns in the range of $-\infty < \mu < \infty$ form the risk-return relationships for the basket, and it is called Markowitz Bullet and depicted in Figure 3.1 for the case of three-asset portfolio. The portfolios that reside on the upper half of the bullet shaped curve are called efficient frontier (Pareto frontier). The minimum risk portfolio with zero return constraint is located on the left most point of the curve and calculated as

$$\mathbf{q} = \frac{\mathbf{C}^{-\mathbf{1}}\mathbf{1}}{\mathbf{1}^{\mathrm{T}}\mathbf{C}^{-\mathbf{1}}\mathbf{1}} \tag{3.15}$$

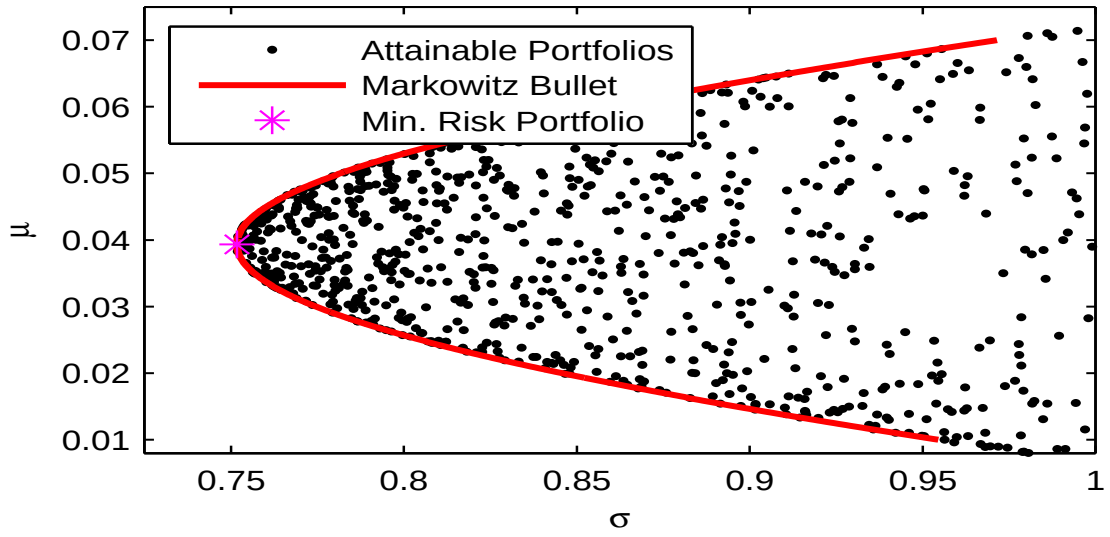

Figure 3.1 Markowitz bullet. All the attainable portfolios ($\mathbf{q}^{\mathrm{T}}\mathbf{1} = 1$) lie on and on the right of the frontier. Portfolios that lie on the upper-half of the Markowitz bullet are called efficient. Minimum risk portfolio is located at the far left tip of the bullet. In this example $\rho_{12} = 0.6$, $\rho_{13} = 0.2$, $\rho_{23} = 0.3$, $\mu_1 = 0.07$, $\mu_2 = 0.03$, and $\mu_3 = 0.02$.

Source: [41].

3.5 Chapter Summary

The framework offered by Modern Portfolio Theory (MPT) is revisited in this chapter. The equations for normalized return of an asset along with its volatility are defined. Expected return and risk of a portfolio are given. Asset return vector of a basket is often modeled as normal (Gaussian) random vector process [43]. The normality assumption makes statistical modeling and analysis tractable although the measurements show that the asset returns do not exactly follow normal distribution. Expected return of a portfolio is defined as weighted combination of expected values of normal random variables. Portfolio risk (volatility) of a portfolio is a function of pair-wise correlations of normal random variables. MPT proposes a solution to portfolio optimization problem that minimizes the risk of a portfolio for a given expected return. In this dissertation, MPT is utilized to evaluate subspace methods used in signal processing applications.

CHAPTER 4

EIGENPORTFOLIOS

Eigenanalysis of covariance matrix describing a random vector process, also called principal component analysis (PCA) or Karhunen-Loeve Transform (KLT) [1, 35, 27, 30, 44, 19], has been successfully employed in many fields including signal processing and quantitative finance. In this chapter, eigenportfolios that are generated from the empirical correlation matrix of asset returns in a basket are focused on. It is emphasized that eigenportfolio returns are perfectly decorrelated. Each eigenvector (EV) generated through the eigendecomposition of an empirical correlation matrix that describes the cross-correlations between asset returns is utilized as an investment allocation vector. For an N-asset basket, eigenanalysis of its empirical correlation matrix for a predefined market history creates N eigenportfolios with their portfolio risks (volatility) and returns. It is noted that signs of eigenvector components bear significant information. A negative component value means a short position for the corresponding asset while a positive one results in a long position.

Market exposure is an important metric for a portfolio and directly related to its market risk. Hence, market-neutrality is a desired feature for lower risk portfolios. Eigenportfolios are considered as a market-neutral investment strategy. They are expected not to be highly affected from the market trend. For a basket of highly correlated assets, its eigenportfolios are almost uncorrelated from the market moves. Except the first eigenportfolio where all positions are long in most cases (high market exposure), the remaining eigenportfolios of a basket with highly correlated assets have relatively low market exposures. In other words, they have built-in self-hedging against market momentum [3]. In contrast, momentum based strategies like index

investing aim to mimic the market where an eigenportfolio with high market exposure may serve the purpose.

It is common to build investment basket where asset returns exhibit high cross-correlations. Portfolios exploit these correlations (co-movements) measured from available market data for a time interval and expressed in empirical correlation matrix of basket. Those correlations dynamically change in time. Hence, the resulting eigenportfolios change in time as well. Asset return vector of a basket is often modeled as normal (Gaussian) random vector process [43]. Although histograms of asset returns for market data show fat-tails, excessive kurtosis and asymmetry properties, the normality assumption makes statistical modeling and analysis tractable. Eigen decomposition perfectly decorrelates given vector process (represented by its covariance matrix) in the eigen subspace where representation coefficients have zero cross-correlations. This property is important and leads to statistical independence of eigen coefficients for Gaussian process. Thus, eigen decomposition of empirical correlation matrix provides its N eigenportfolios with perfectly decorrelated portfolio returns. Those uncorrelated returns are particularly used as independent variables of regression for predictions of individual asset returns in mean reversion based trading strategies [2, 3].

In this chapter, performances of eigenportfolio returns for autoregressive discrete process of order one, AR(1) are analyzed, by using financial metrics like Sharpe ratio (risk-adjusted return) and market exposure. Then, a method is proposed to design optimized super eigenportfolio (OSEP) that is comprised of multiple eigenportfolios with optimal weights that represent their investment allocations.

4.1 Eigenanalysis and Eigenportfolios of Empirical Correlation Matrix

PCA (KLT) is the optimal subspace (transform) method and also used to create eigenportfolios [2, 1]. Eigenanalysis of covariance (empirical correlation) matrix $\mathbf{C}$

of asset returns in a basket yields a set of eigenportfolios with perfectly decorrelated returns. The built-in decorrelation property of eigenportfolio returns is a desirable feature since performance of a particular eigenportfolio has no effect on other eigenportfolios. This property makes eigenportfolios to comply with the theory (with the Gaussian assumption) and used as independent variables of regression analysis employed in quantitative trading strategies like statistical arbitrage [3]. Moreover, except the first eigenportfolio with long only positions in a typical scenario, eigenportfolios offer market-neutrality whenever their eigenvectors (capital allocations with long and short positions) have zero mean. It is noted that a market neural portfolio is self-hedged against market fluctuations and employed in low-risk investment strategies. The design steps of eigenportfolios are summarized as follows.

Each asset return in asset return vector $\mathbf{r}$ is normalized to be zero mean and unit variance as

$$\begin{aligned} \widehat{\mathbf{r}} &= [\widehat{r_k}]\,; k = 1, 2, \ldots, N \\ \widehat{r_k} &= \frac{r_k - \mu_k}{\sigma_k} \end{aligned} \tag{4.1}$$

where μ_k and σ_k are its mean and standard deviation, respectively. The covariance (correlation) matrix ($\mathbf{C} = \mathbf{R}$ due to normalization) of asset returns is expressed as

$$\begin{aligned} \mathbf{R}_E &\triangleq \left[E\left\{\widehat{\mathbf{r}}\widehat{\mathbf{r}}^T\right\}\right] = [R_{k,l}] \\ &= \begin{bmatrix} R_{1,1} & R_{1,2} & \cdots & R_{1,N} \\ R_{2,1} & R_{2,2} & \cdots & R_{2,N} \\ \vdots & \vdots & \ddots & \vdots \\ R_{N,1} & R_{N,2} & \cdots & R_{N,N} \end{bmatrix} \end{aligned} \tag{4.2}$$

where its elements

$$R_{k,l} = E\left\{\widehat{r}_k \widehat{r}_l\right\} = \frac{1}{W}\sum_{m=0}^{W-1} \widehat{r}_k(n-m)\widehat{r}_l(n-m) \tag{4.3}$$

represent measured cross-correlations for an observation (time) window of W samples. $\mathbf{R}_E$ is assumed to be a real, symmetric and positive definite matrix. The eigendecomposition of $\mathbf{R}_E$ as defined in (2.15) is written as [1, 44]

$$\mathbf{R}_E = \mathbf{A}_{KLT}^T \mathbf{\Lambda} \mathbf{A}_{KLT} = \sum_{k=1}^{N} \lambda_k \boldsymbol{\phi}_k \boldsymbol{\phi}_k^T \tag{4.4}$$

where $\{\lambda_k, \boldsymbol{\phi}_k\}$ are eigenvalue-eigenvector pairs.

Since asset returns are not variance stationary in real life, it is common to normalize asset risks during the creation of eigenportfolios. Hence, eigenportfolio returns with such a normalization are calculated as [41, 3]

$$\mathbf{r}^{ep} = \boldsymbol{\theta} = \widetilde{\mathbf{A}}_{KLT}^T \mathbf{r} \tag{4.5}$$

where $\widetilde{\mathbf{A}}_{KLT}$ is comprised of eigenvectors defined as

$$\begin{aligned} \widetilde{\boldsymbol{\phi}}_k &= \left[\widetilde{\boldsymbol{\phi}}_k^{(i)}\right]; i = 1, 2, \ldots, N \\ \widetilde{\boldsymbol{\phi}}_k^{(i)} &= \frac{\boldsymbol{\phi}_k^{(i)}}{\sigma_i} \end{aligned} \tag{4.6}$$

Eigenportfolio risks (volatilities) are expressed as [41]

$$\begin{aligned} \boldsymbol{\sigma}^{ep} &= \boldsymbol{\sigma}_\theta = \left[\sigma_{\theta_k}\right]; k = 1, 2, \ldots, N \\ \sigma_k^{ep} &= \sigma_{\theta_k} = \sqrt{\lambda_k} = \left(\boldsymbol{\phi}_k^{\mathbf{T}} \mathbf{R}_E \boldsymbol{\phi}_k\right)^{1/2} \end{aligned} \tag{4.7}$$

Therefore, the Sharpe ratio of the kth eigenportfolio is calculated as follows

$$\boldsymbol{S}^{ep} = \boldsymbol{S}_{\theta} = [S_{\theta_k}]\,; k = 1, 2, \ldots, N$$
$$S_k^{ep} = S_{\theta_k} = \frac{\mu_{\theta_k}}{\sigma_{\theta_k}} \tag{4.8}$$

where $\mu_{\theta_k} = E\{\theta_k\}$. Market exposure (unhedged against market fluctuations) of eigenportfolios are defined as

$$\boldsymbol{M}^{ep} = [M_k^{ep}]\,; k = 1, 2, \ldots, N$$
$$M_k^{ep} = \sum_{i=1}^{N} \boldsymbol{\phi}_k^{(i)} \tag{4.9}$$

where M_k^{ep} is the market exposure of the kth eigenportfolio.

4.2 Eigenportfolio Returns for AR(1) Process

In this section, eigenportfolio returns are formulated and expressions are derived for their performance. Although asset returns have mean and variance non-stationarity in reality, stationarity is assumed [43]. Asset return vector $\mathbf{r}$ of a basket at time n is modeled as autoregressive discrete vector process with order one, AR(1). AR(1) with finite dimension and $-1 < \rho < 1$ is considered as Gaussian random process with constant mean and variance [21]. For simplicity, it is assumed to have unit variance. It has a kernel for its eigenportfolios [40]. $\mathbf{R_x}$ is an $N \times N$ correlation matrix defined in (2.6) for a given ρ. The resulting eigenportfolio returns are calculated as

$$\mathbf{r}^{ep} = \boldsymbol{\theta} = \mathbf{A}_{KLT}^{T}\mathbf{r} \tag{4.10}$$

Therefore, each KLT coefficient is equivalent to the return of its corresponding eigenportfolio with independent normal distribution, $\{\theta_k \sim N(\mu_{\boldsymbol{\theta}_k}, \lambda_k)\}\,\forall k$ where λ_k is the kth eigenvalue. Its mean, $\mu_{\boldsymbol{\theta}_k}$, is defined as

$$\mu_{\boldsymbol{\theta}_k} = E\{\theta_k\} = \sum_{i=1}^{N} E\{\mathbf{r}_i\}\,\boldsymbol{\phi}_k^{(i)} \tag{4.11}$$

The components of $\boldsymbol{\theta}$ have the inherent perfect decorrelation property written as [1]

$$E\{\theta_j\theta_k\} = \sigma^2_{\boldsymbol{\theta}_j}\delta(j-k) \tag{4.12}$$

When the random vector process has multivariate normal distribution with zero mean and unit variance, the representation (transform) coefficients $\{\theta_k\}$ are statistically independent normal random variables [28]. Thus, their joint probability density function (pdf) is defined as

$$f_{\theta_1,\theta_2,\ldots,\theta_N}(\theta_1,\theta_2,\ldots,\theta_N) = f_{\theta_1}(\theta_1)\,f_{\theta_2}(\theta_2)\ldots f_{\theta_N}(\theta_N) \tag{4.13}$$

where

$$\left\{ f_{\theta_k}(\theta_k) = \frac{1}{\sigma^2_{\boldsymbol{\theta}_k}\sqrt{2\pi}} e^{-\frac{\left(\theta_k-\mu_{\boldsymbol{\theta}_k}\right)^2}{2\sigma^2_{\boldsymbol{\theta}_k}}} \right\} \forall k \tag{4.14}$$

It is noted that signal dependent KLT optimally repacks signal energy in the subspace. It maximizes the ratio [1]

$$G_{TC} = \frac{\frac{1}{N}\sum_{k=1}^{N}\sigma^2_{\boldsymbol{\theta}_k}}{\left(\prod_{k=1}^{N}\sigma^2_{\boldsymbol{\theta}_k}\right)^{1/N}} \tag{4.15}$$

This property implies maximized unevenness among squared volatilities of eigenportfolios.

Since the mean of AR(1) process is constant, the mean, volatility, and Sharpe ratio, S_k, for the return of the kth eigenportfolio (transform coefficient) are calculated as follows

$$\mu_{\boldsymbol{\theta}_k} = E\left\{\theta_k\right\} = M_k \mu_{\mathbf{x}} = \boldsymbol{\phi}_k^A \mu_{\mathbf{x}} = \boldsymbol{\phi}_k^A \frac{c}{1-\rho} \tag{4.16}$$

$$\sigma_{\boldsymbol{\theta}_k} = \left(E\left\{\theta_k^2\right\} - \mu_{\boldsymbol{\theta}_k}^2\right)^{1/2} = \sqrt{\lambda_k} = \left(\boldsymbol{\phi}_k^T \mathbf{R}_{\mathbf{x}} \boldsymbol{\phi}_k\right)^{1/2} \tag{4.17}$$

$$S_k = \frac{\mu_{\boldsymbol{\theta}_k}}{\sigma_{\boldsymbol{\theta}_k}} \tag{4.18}$$

where

$$M_k = \boldsymbol{\phi}_k^A = \sum_{i=1}^{N} \boldsymbol{\phi}_k^{(i)} \tag{4.19}$$

It is emphasized that the mean of the kth eigenportfolio return, $\{\mu_{\boldsymbol{\theta}_k}\}$, for AR(1) process depends on the constant c (market trend), correlation coefficient ρ, and its market exposure, M_k, as shown in (4.16). Note that M_k is also a function of ρ. This expression suggests that one should form a basket of assets with highly correlated historical returns in order to generate eigenportfolios with good returns. (4.16) shows that market trend, c, and market exposure of an eigenportfolio, M_k, are also important factors for its return. Moreover, this equation shows that the expected values of eigenportfolio returns are zero, $\{\mu_{\boldsymbol{\theta}_k} = 0\}\,\forall k$, whenever there is no trend in the market, $c = 0$, or eigenportfolio has no market exposure, $M_k = 0$. On the other hand, for $M_k \neq 0$ and $c \neq 0$, means of eigenportfolio returns are dictated by their market exposures and the market trend. The market exposure M_k and the market

trend c dominate the return of an eigenportfolio for a given correlation coefficient ρ. It is an interesting observation from (2.20) that the even indexed eigenvectors of AR(1) process have zero-mean when $\rho > 0$, hence, $M_k = 0$. The odd indexed eigenvectors have also zero-mean when $\rho < 0$. Thus, the returns of these eigenportfolios are zero regardless of the values of c and ρ.

In a real world scenario, the means of asset returns are varying in time and not the same for all assets in the basket. In order to make the model more realistic, the constant c in AR(1) model, (2.1), is also assumed as a random variable with normal distribution, $c \sim N(\mu_c, \sigma_c^2)$. Therefore, μ_x has normal distribution as well, $\mu_x \sim N\left(\frac{\mu_c}{1-\rho}, \frac{\sigma_c^2}{(1-\rho)^2}\right)$. The mean values and Sharpe ratios of eigenportfolio returns defined in (4.16) and (4.18), respectively, are considered as random variables. The mean of the kth eigenportfolio return for constant ρ has the normal distribution as follows

$$\mu_{\boldsymbol{\theta}_k} \sim N\left(\mu_{\mu_{\boldsymbol{\theta}_k}}, \sigma^2_{\mu_{\boldsymbol{\theta}_k}}\right) \tag{4.20}$$

where $\mu_{\mu_{\boldsymbol{\theta}_k}}$ and $\sigma^2_{\mu_{\boldsymbol{\theta}_k}}$ are defined as

$$\begin{aligned} \mu_{\mu_{\boldsymbol{\theta}_k}} &= E\left\{\mu_{\boldsymbol{\theta}_k}\right\} \\ &= \boldsymbol{\phi}_k^A E\left\{\mu_x\right\} \\ &= \boldsymbol{\phi}_k^A \frac{\mu_c}{1-\rho} \end{aligned} \tag{4.21}$$

and

$$\begin{aligned} \sigma^2_{\mu_{\boldsymbol{\theta}_k}} &= E\left\{\mu^2_{\boldsymbol{\theta}_k}\right\} - \mu^2_{\mu_{\boldsymbol{\theta}_k}} \\ &= \left(\boldsymbol{\phi}_k^A\right)^2 \left(E\left\{\mu_x^2\right\} - \mu_x^2\right) \\ &= \left(\boldsymbol{\phi}_k^A\right)^2 \frac{\sigma_c^2}{(1-\rho)^2} \end{aligned} \tag{4.22}$$

Sharpe ratio of each eigenportfolio also has normal distribution as

$$S_k \sim N\left(\mu_{S_k}, \sigma^2_{S_k}\right) \tag{4.23}$$

where μ_{S_k} and $\sigma^2_{S_k}$ are calculated as follows

$$\begin{aligned} \mu_{S_k} &= E\left\{S_k\right\} \\ &= \left(\frac{\boldsymbol{\phi}_k^A}{\sqrt{\lambda_k}}\right) E\left\{\mu_x\right\} \\ &= \left(\frac{\boldsymbol{\phi}_k^A}{\sqrt{\lambda_k}}\right) \frac{\mu_c}{1-\rho} \end{aligned} \tag{4.24}$$

$$\begin{aligned} \sigma^2_{S_k} &= E\left\{S_k^2\right\} - \mu^2_{S_k} \\ &= \left(\frac{\boldsymbol{\phi}_k^A}{\sqrt{\lambda_k}}\right)^2 \left(E\left\{\mu_x^2\right\} - \mu_x^2\right) \\ &= \left(\frac{\boldsymbol{\phi}_k^A}{\sqrt{\lambda_k}}\right)^2 \frac{\sigma_c^2}{(1-\rho)^2} \end{aligned} \tag{4.25}$$

It is validated in Section 4.4 that the proposed framework to calculate eigenportfolio performance for AR(1) model through an example where actual market data is used.

4.3 Super Eigenportfolio

The design of eigenportfolios for AR(1) process is extended in this section. Herein, the problem of allocating the total investment among eigenportfolios is looked into in order to maximize the overall financial performance. Hence, the resulting investment portfolio is called as super eigenportfolio (SEP). Although a simple way to allocate total investment among eigenportfolios is to assign even amount (Talmudic allocation) to each eigenportfolio ($\left\{\alpha_k = \frac{1}{N}\right\} \forall k$), the task is stated as an optimal capital allocation problem and it is presented in the next section.

With the assumptions that all eigenportfolios are considered for investment and $\mathbf{r}$ has multivariate normal distribution of unit variance, the return of a super eigenportfolio, θ_{SEP}, is defined as

$$\theta_{SEP} = \sum_{k=1}^{N} \alpha_k \theta_k = \sum_{k=1}^{N} \sum_{i=1}^{N} \alpha_k \boldsymbol{\phi}_k^{(i)} \mathbf{r}_i \tag{4.26}$$

where $\sum_{k=1}^{N} \alpha_k = 1$. θ_{SEP} is a linear combination of independent normal random variables (eigenportfolio returns). Thus, it has a normal distribution, $\theta_{SEP} \sim N\left(\mu_{\theta_{SEP}}, \sigma^2_{\theta_{SEP}}\right)$. The mean, volatility and Sharpe ratio of the resulting super eigenportfolio is defined as [28]

$$\mu_{\theta_{SEP}} = E\left\{\theta_{SEP}\right\} = \sum_{k=1}^{N} \alpha_k \mu_{\theta_k} \tag{4.27}$$

$$\sigma_{\theta_{SEP}} = \left(E\left\{\theta^2_{SEP}\right\} - \mu^2_{\theta_{SEP}}\right)^{1/2} = \left(\sum_{k=1}^{N} \alpha_k^2 \sigma^2_{\theta_k}\right)^{1/2} \tag{4.28}$$

$$S_{SEP} = \frac{\mu_{\theta_{SEP}}}{\sigma_{\theta_{SEP}}} \tag{4.29}$$

Similarly, the market exposure of SEP is calculated as

$$M_{SEP} = \sum_{k=1}^{N} \alpha_k \boldsymbol{\phi}_k^A \tag{4.30}$$

4.3.1 Optimized Super Eigenportfolio (OSEP)

The Sharpe ratio of super eigenportfolio, S_{SEP}, is used as the metric for optimal allocation of the total investment among eigenportfolios. The formulation of the problem is given as follows

$$\begin{aligned} \max \quad & S_{SEP} \\ \textbf{s.t.} \quad & \sum_{k=1}^{N} \alpha_k = 1 \end{aligned} \tag{4.31}$$

Maximizing Sharpe ratio is a multiobjective optimization problem (Pareto optimization). Risk (volatility) defined in (4.28) has to be minimized while the mean, (4.27), is maximized. There is no single solution that simultaneously optimizes both objective functions. In such a case, Pareto optimal (Pareto efficient) solutions or efficient frontier are generated in order to obtain the solution that maximizes S_{SEP}. Pareto optimal solutions are the ones that none of the objective functions can be improved without making at least one of the objective functions worsening [18]. One way to generate Pareto optimal solutions for this problem is to convert the multiobjective problem into a single objective optimization problem by assigning only positive weights to each objective function [18]. The standard method is defined as

$$\min \quad F(\mathbf{x}) = \sum_{k=1}^{N} \nu_k f_k(\mathbf{x}) \tag{4.32}$$

where $\nu_k > 0;\ k = 1, 2, \ldots, N$. By tuning the weights, $\{\nu_k\}$, the Pareto optimal solutions can be generated.

The multiobjective optimization problem defined in (4.31) is converted into a single objective optimization problem and expressed as

$$\begin{aligned} \min \quad & \nu_1 \left(\sum_{k=1}^{N} \alpha_k^2 \sigma_{\theta_k}^2 \right)^{1/2} - \nu_2 \sum_{k=1}^{N} \alpha_k \mu_{\theta_k} \\ \textbf{s.t.} \quad & \sum_{k=1}^{N} \alpha_k = 1 \end{aligned} \tag{4.33}$$

where $0 \leq \nu_1, \nu_2 \leq 1$ and $\nu_1 + \nu_2 = 1$. Among the Pareto optimal solutions, the one that maximizes the Sharpe ratio is selected as the solution for the optimization problem of (4.31). The optimization problem in (4.33) can be solved by use of numerical methods currently available.

If the problem is modified to minimize variance (similar to MPT) rather than standard deviation and stated as

$$\begin{aligned} \min \quad & \nu_1 \sum_{k=1}^{N} \alpha_k^2 \sigma_{\theta_k}^2 - \nu_2 \sum_{k=1}^{N} \alpha_k \mu_{\theta_k} \\ \mathbf{s.t.} \quad & \sum_{k=1}^{N} \alpha_k = 1 \end{aligned} \tag{4.34}$$

an analytical solution is derived. The multiobjective optimization of (4.34) is a quadratic optimization problem stated as

$$\begin{aligned} \min \quad & \nu_1 \boldsymbol{\alpha}^{\boldsymbol{T}} \mathbf{V} \boldsymbol{\alpha} - \nu_2 \boldsymbol{\alpha}^{\boldsymbol{T}} \boldsymbol{\mu}_\theta \\ \mathbf{s.t.} \quad & \mathbf{1^T} \boldsymbol{\alpha} = 1 \end{aligned} \tag{4.35}$$

where $\left\{\sigma_{\theta_k}^2\right\}$ and $\{\mu_{\theta_k}\}$ populate the diagonal matrix $\mathbf{V}$ and vector $\boldsymbol{\mu}_\theta$, respectively. ν_1 and ν_2 are the tuning parameters for Pareto frontier. In quadratic programming, the optimization problem is convex when $\mathbf{V}$ is a positive-definite matrix [10]. Since $\mathbf{V}$ is diagonal with positive elements, it is a positive-definite matrix. Hence, the optimization problem in (4.35) is convex.

Using Lagrangian multiplier, the multiobjective optimization problem is modified as follows

$$\mathcal{L}(\boldsymbol{\alpha}, \beta) = \nu_1 \sum_{k=1}^{N} \alpha_k^2 \sigma_{\theta_k}^2 - \nu_2 \sum_{k=1}^{N} \alpha_k \mu_{\theta_k} + \beta \left(\sum_{k=1}^{N} \alpha_k - 1 \right) \tag{4.36}$$

Then,

$$\frac{\partial \mathcal{L}\left(\boldsymbol{\alpha}, \beta\right)}{\partial \alpha_k} = 0 \tag{4.37}$$

$$-\nu_2 \mu_{\theta_k} + 2\nu_1 \sigma_{\theta_k}^2 \alpha_k + \beta = 0 \tag{4.38}$$

$$\alpha_k = \frac{\left(\nu_2 \mu_{\theta_k} - \beta\right) \sigma_{\theta_k}^{-2}}{2\nu_1} \tag{4.39}$$

$$\boldsymbol{\alpha} = \frac{\mathbf{V^{-1}} \left[\nu_2 \boldsymbol{\mu}_\theta - \beta\right]}{2\nu_1} \tag{4.40}$$

To solve the Lagrangian multiplier, we substitute (4.39) in the constraint of (4.35)

$$\sum_{k=1}^{N} \frac{\left(\nu_2 \mu_{\theta_k} - \beta\right) \sigma_{\theta_k}^{-2}}{2\nu_1} = 1 \tag{4.41}$$

$$\sum_{k=1}^{N} \frac{\nu_2 \mu_{\theta_k} \sigma_{\theta_k}^{-2}}{2\nu_1} - \sum_{k=1}^{N} \frac{\beta \sigma_{\theta_k}^{-2}}{2\nu_1} = 1 \tag{4.42}$$

$$\sum_{k=1}^{N} \frac{\nu_2 \mu_{\theta_k} \sigma_{\theta_k}^{-2}}{2\nu_1} - 1 = \beta \sum_{k=1}^{N} \frac{\sigma_{\theta_k}^{-2}}{2\nu_1} \tag{4.43}$$

$$\beta = \frac{\left(\sum_{k=1}^{N} \nu_2 \mu_{\theta_k} \sigma_{\theta_k}^{-2}\right) - 2\nu_1}{\sum_{i=1}^{N} \sigma_{\theta_k}^{-2}} \tag{4.44}$$

$$\beta = \frac{\nu_2 \mathbf{1^T V^{-1}} \boldsymbol{\mu}_\theta - 2\nu_1}{\mathbf{1^T V^{-1} 1}} \tag{4.45}$$

$$\begin{aligned} \boldsymbol{\alpha} &= \frac{\mathbf{V^{-1}} \left[\nu_2 \boldsymbol{\mu}_\theta - \beta\right]}{2\nu_1} \\ \beta &= \frac{\nu_2 \mathbf{V^{-1}} \boldsymbol{\mu}_\theta - 2\nu_1}{\mathbf{V^{-1} 1}} \end{aligned} \tag{4.46}$$

where $\left\{\sigma^2_{\theta_k}\right\}$ and $\{\mu_{\theta_k}\}$ populate the diagonal elements of matrix $\mathbf{V}$ and components of vector $\boldsymbol{\mu}_\theta$, respectively. ν_1 and ν_2 are the tuning parameters for Pareto frontier. $\mathbf{1}$ is the $N \times 1$ unit vector, $\mathbf{1^T} = \begin{bmatrix} 1 & 1 & \cdots & 1 \end{bmatrix}$.

4.4 Performance of Eigenportfolios for AR(1) Process

Eigenportfolios of AR(1) process are evaluated with respect to Sharpe ratios of their returns and also their market exposures. Moreover, the empirical correlation matrix for a basket of four stocks is measured from market data and approximated it by an AR(1) process to validate the proposed framework.

4.4.1 Eigenportfolios of AR(1) Process

The market exposures, ϕ^A, and expected values of Sharpe ratios, μ_S, for the first and the last five odd indexed eigenportfolios of AR(1) process, with $\mu_c = 1$ bps and size $N = 30$, as a function of ρ are displayed in Figure 4.1a and 4.1b, respectively. ϕ^A and μ_S of optimized super eigenportfolio (OSEP) are also included in these figures. First eigenportfolio has *long* positions for all assets. Therefore, it has the highest market exposure and its expected Sharpe ratio increases when ρ gets higher. In contrast, an eigenportfolio with the zero sum of its *long* and *short* positions has no market exposure. It is observed from Figure 4.1a that odd indexed eigenportfolios have zero market exposure for $\rho < 0$. Hence, their Sharpe ratios are zero. Similarly, Figure 4.2a

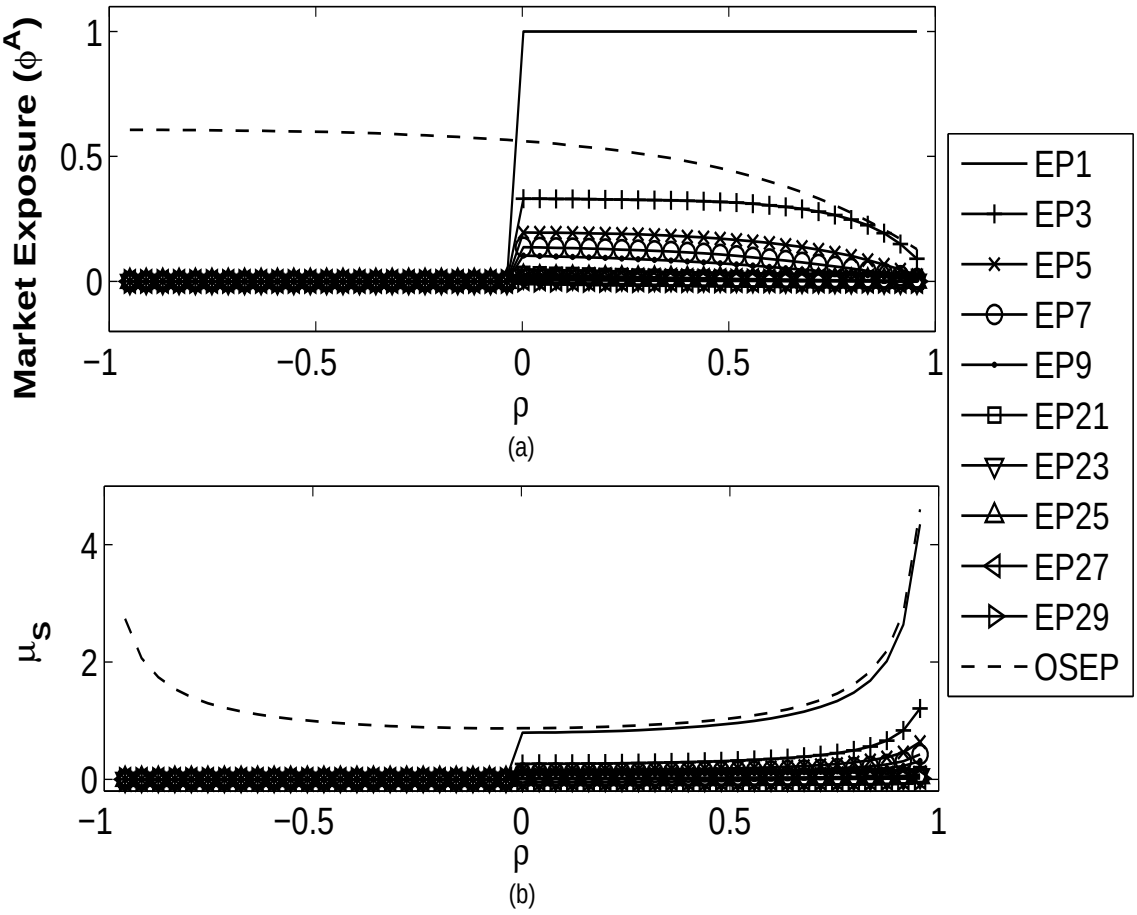

Figure 4.1 (a) Market exposures, $\boldsymbol{\phi}^A$, and (b) expected values of Sharpe ratios, μ_S, for the first and the last five odd indexed eigenportfolios (EPs) of AR(1) process along with optimized super eigenportfolio (OSEP) for $\mu_c = 1$ bps and $N = 30$ with respect to ρ.

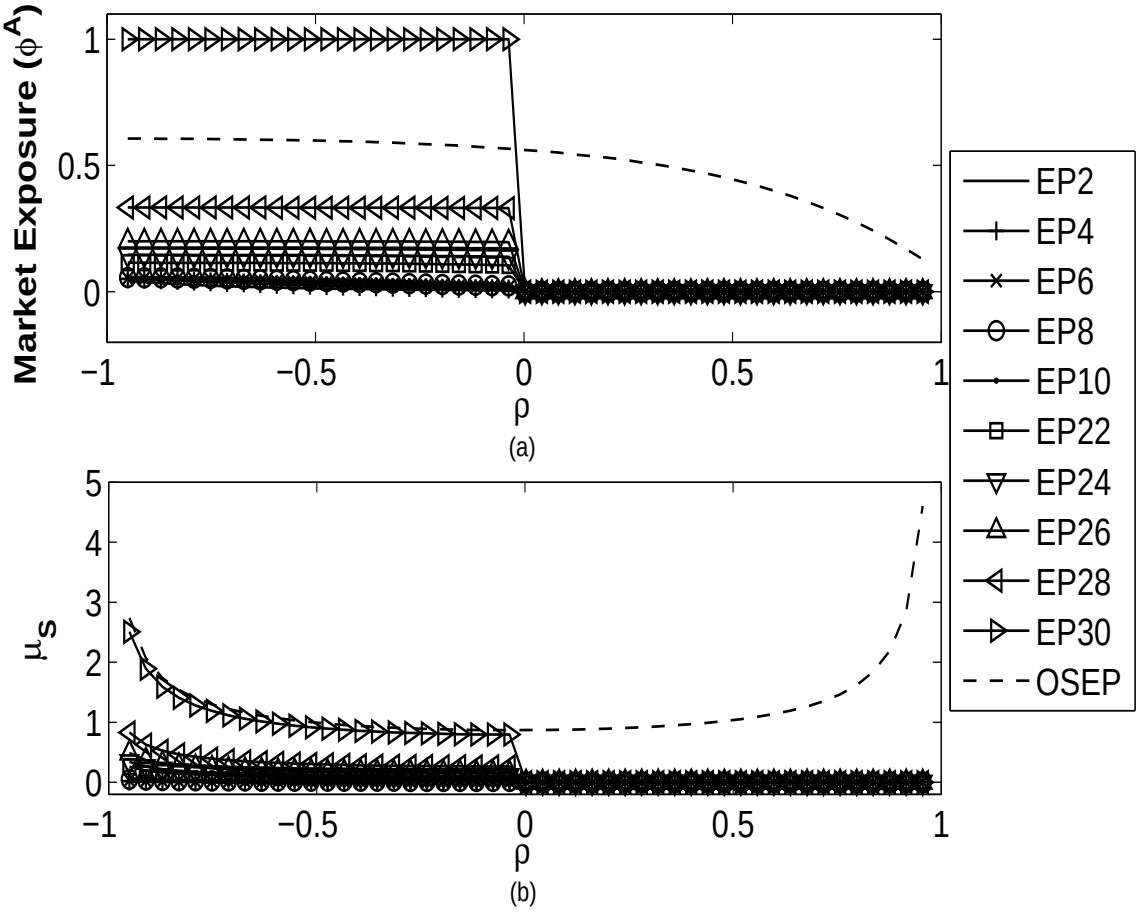

Figure 4.2 (a) Market exposures, $\boldsymbol{\phi}^A$, and (b) expected values of Sharpe ratios, μ_S, for the first and the last five even indexed eigenportfolios (EPs) of AR(1) process along with optimized super eigenportfolio (OSEP) for $\mu_c = 1$ bps and $N = 30$ with respect to ρ.

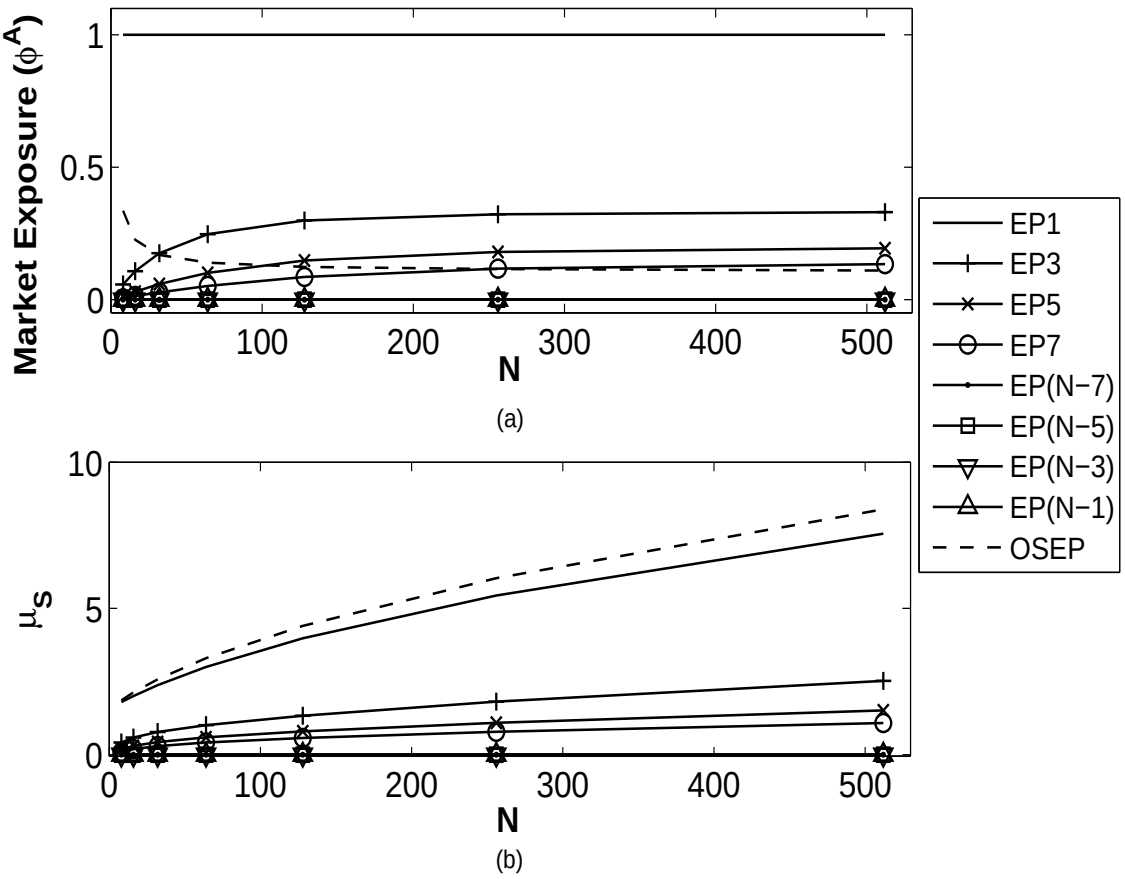

Figure 4.3 (a) Market exposures, $\boldsymbol{\phi}^A$, and (b) expected values of Sharpe ratios, μ_S, for the first and the last four odd indexed eigenportfolios (EPs) of AR(1) process along with optimized super eigenportfolio (OSEP) for $\mu_c = 1$ bps and $\rho = 0.9$ with respect to the size N.

and 4.2b display the ϕ^A and μ_S of the first and last five even indexed eigenportfolios, respectively. The last eigenportfolio performs the best for $\rho < 0$. It is noted that the market exposure of OSEP decreases as ρ goes to one. Moreover, it provides the best Sharpe ratio among all eigenportfolios for all the cases considered.

The market exposures, ϕ^A, and expected values of Sharpe ratios, μ_S, for the first and the last four odd indexed eigenportfolios of AR(1) process, with $\mu_c = 1$ bps and $\rho = 0.9$, and OSEP as a function of size N are displayed in Figure 4.3a and 4.3b, respectively. The expected Sharpe ratios of eigenportfolios with non-zero market exposures increase with portfolio size where OSEP performs the best among

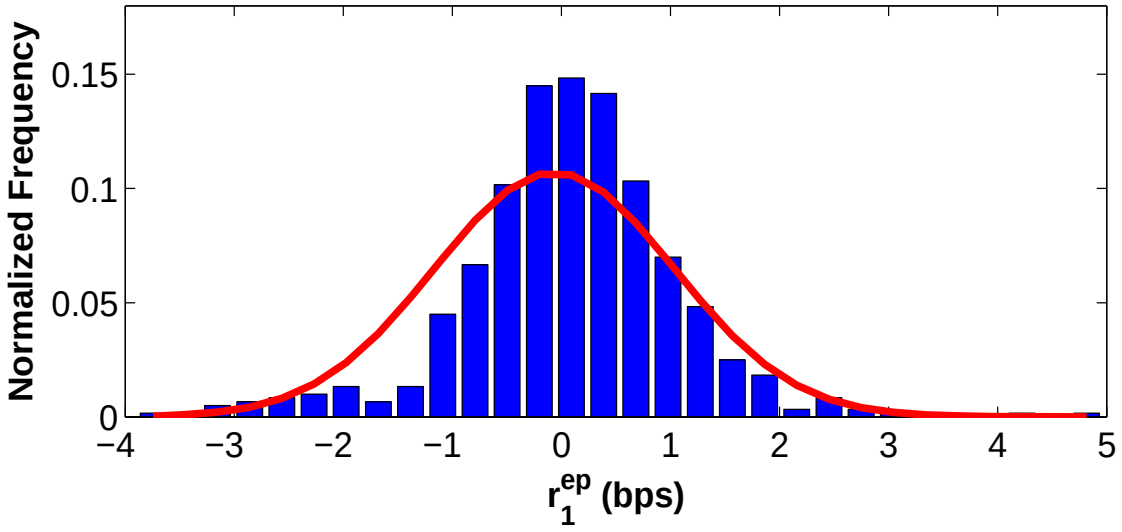

Figure 4.4 Normalized histogram of end of day (EOD) returns for the first eigenportfolio (EP1) derived from empirical correlation matrix of the basket {MMM, UTX, PFE, UNH}, $N = 4$, with $W = 600$ days ending on January 24, 2014 along with the Gaussian pdf of the mean and standard deviation calculated from (4.16) and (4.17), respectively. The AR(1) model parameters of (2.1) for this set of market data are estimated as $c = 0.02$ bps and $\rho = 0.75$. The mean, standard deviation and Sharpe ratio of the histogram are calculated as $\mu^m_{\boldsymbol{\theta}_1} = 0.081$ bps, $\sigma^m_{\boldsymbol{\theta}_1} = 1.06$ bps, and $S^m_1 = 1.122$, respectively, for the AR(1) model. Similarly, they are calculated as $\mu^d_{\boldsymbol{\theta}_1} = 0.082$ bps, $\sigma^d_{\boldsymbol{\theta}_1} = 0.98$ bps, and $S^d_1 = 1.328$ for the market data. It is noted that the same eigenportfolio is used to calculate its in-sample EOD returns for the entire duration of $W = 600$ days.

all the cases considered. Similar trend is observed for various ρ values. On the other hand, the market exposure is significantly less sensitive to the size in particular when $N >$200.

4.4.2 Eigenportfolios of a Basket

A basket of four stocks {MMM, UTX, PFE, UNH} is created to validate the proposed framework by evaluating its eigenportfolio returns. Their end of day (EOD) returns are used in this study. The empirical correlation matrix is calculated and its eigenanalysis is performed. Large window sizes resulted in comparable values for mean and variance of asset returns, and a good AR(1) approximation to market data

Table 4.1 Mean, Standard Deviation and Annual Sharpe Ratios of End of Day (EOD) Returns for In-Sample Eigenportfolios

		EP1	EP2	EP3	EP4
$\mu_{\boldsymbol{\theta}_k}$(bps)	AR(1)	0.081	0.0	-0.005	0.00
	Data	0.082	-0.002	-0.012	-0.003
$\sigma_{\boldsymbol{\theta}_k}$(bps)	AR(1)	1.06	0.54	0.32	0.27
	Data	0.98	0.66	0.48	0.37
S_k (annual)	AR(1)	1.122	0.00	-0.251	0.00
	Data	1.328	-0.068	-0.411	-0.14

Table 4.2 Mean, Standard Deviation and Annual Sharpe Ratios of End of Day (EOD) Returns for Out-Sample Eigenportfolios

		EP1	EP2	EP3	EP4
$\mu_{\boldsymbol{\theta}_k}$(bps)	AR(1)	0.074	0.0	-0.003	0.00
	Data	0.072	-0.003	-0.0	-0.012
$\sigma_{\boldsymbol{\theta}_k}$(bps)	AR(1)	0.93	0.4	0.23	0.19
	Data	0.75	0.62	0.54	0.34
S_k (annual)	AR(1)	1.27	0.00	-0.23	0.00
	Data	1.54	-0.085	-0.007	-0.57

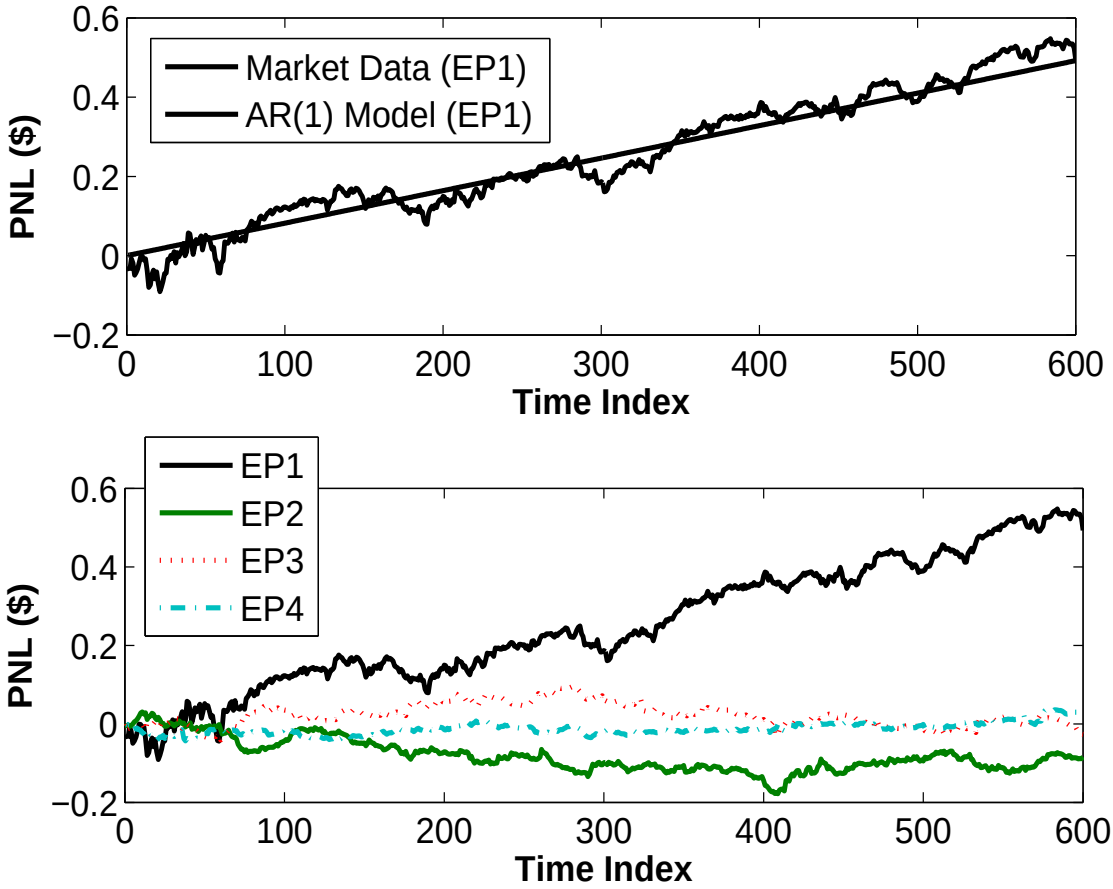

Figure 4.5 Profit and Loss (PNL) curves of end of day (EOD) returns for (a) the first eigenportfolio, and (b) the four eigenportfolios, generated from empirical correlation matrix of the basket {MMM, UTX, PFE, UNH}, $N = 4$, with $W = 600$ days ending on January 24, 2014. The linear PNL curve generated for the first eigenportfolio of AR(1) process per (4.16) and for the parameters $c = 0.02$ bps and $\rho = 0.75$ is also displayed in (a) to highlight the model fit.

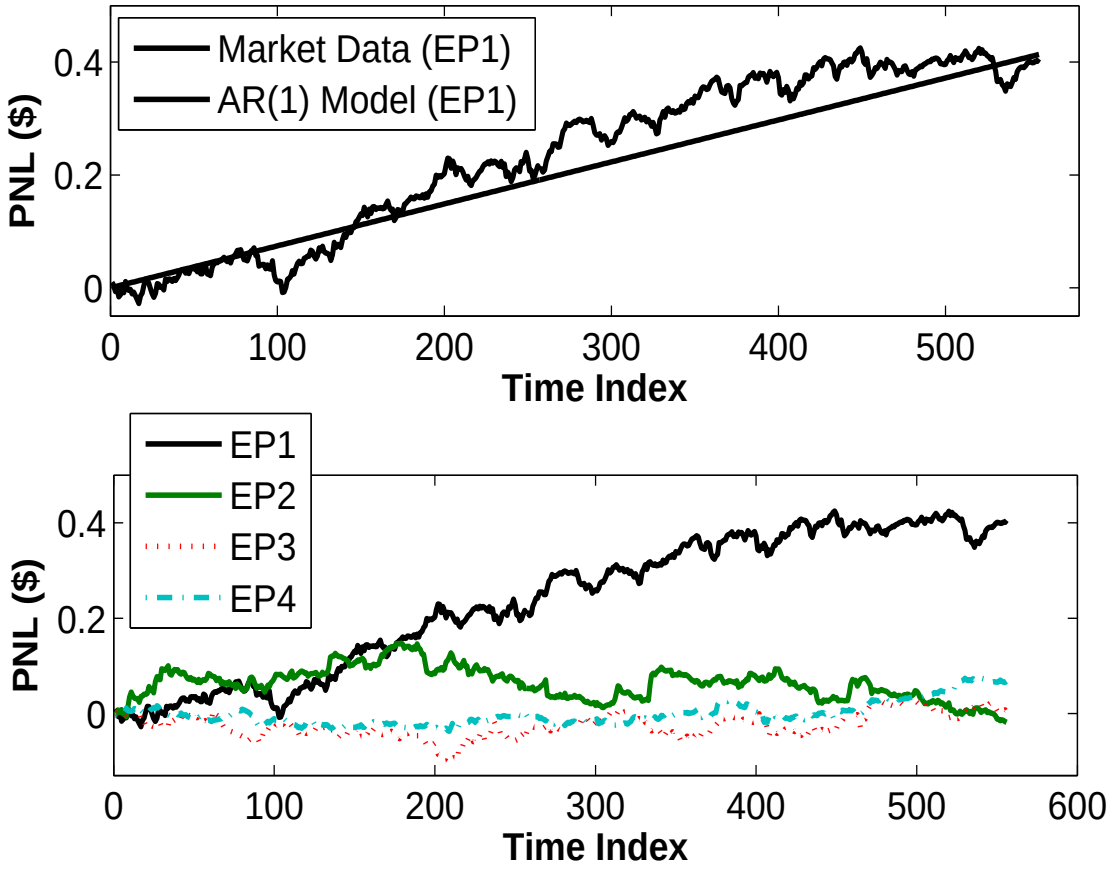

Figure 4.6 (a) Profit and Loss (PNL) curves of end of day (EOD) returns for the out-sample first eigenportfolio generated from empirical correlation matrix of the basket {MMM, UTX, PFE, UNH}, $N = 4$, with $W = 200$ days ending on June 19, 2012 and 556 days out of sample market data ending on September 5, 2014. The linear PNL curve generated for the first eigenportfolio of AR(1) process per (4.16) and for the parameters $c = 0.013$ bps and $\rho = 0.81$ is also displayed to highlight the model fit. (b) Profit and Loss (PNL) curves of end of day (EOD) returns for all eigenportfolios.

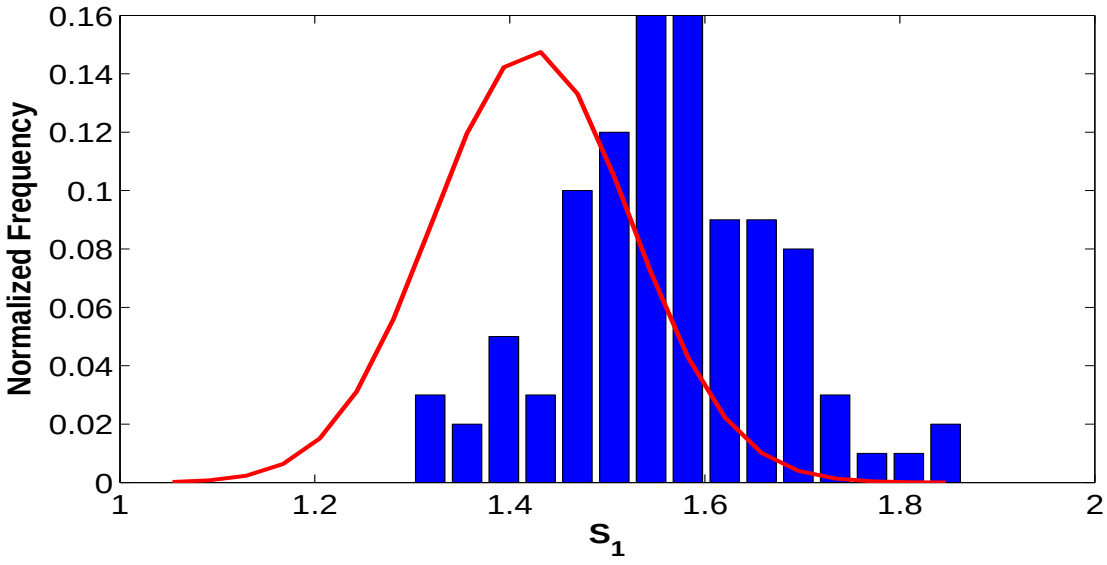

Figure 4.7 Normalized histogram of in-sample annual Sharpe ratios measured between January 24, 2014 and June 18, 2014 for the EOD returns of the first eigenportfolio created for the empirical correlation matrix of a basket {MMM, UTX, PFE, UNH}, $N = 4$, for the measurement window of $W = 600$ days along with Gaussian pdf of mean and standard deviation calculated from (4.24) and (4.25), respectively. The AR(1) model parameters of (2.1) are estimated as $\mu_c = 1.73$ bps and $\rho = 0.77$. The mean and standard deviation of the histogram are calculated as $\mu^d_{S_k} = 1.59$ and $\sigma^d_{S_k} = 0.108$, respectively. Similarly, they are calculated as $\mu^m_{S_k} = 1.47$ and $\sigma^m_{S_k} = 0.09$ for the AR(1) model. It is noted that c in (2.1) is itself a Gaussian random variable with $N\left(\mu_c = 1.73\, bps, \sigma_c^2 = 0.0001\, bps\right)$ for this market data.

with W=600 is obtained for that stock basket. It is assumed that \$1 investment in each eigenportfolio and no transaction cost is considered.

Figure 4.7a displays the normalized histogram of the EOD returns for the first eigenportfolio (EP1) generated from the empirical correlation matrix, $W = 600$, of four-stock basket {MMM, UTX, PFE, UNH} for the market data ending on January 24, 2014. In addition, Gaussian pdf with $\mu^m_{\boldsymbol{\theta}_1} = 0.081$ bps, $\sigma^m_{\boldsymbol{\theta}_1} = 1.06$ bps is also displayed in this figure. c in AR(1) model is assumed to be constant. AR(1) model parameters are measured from market data as $c = 0.02$ bps and $\rho = 0.75$. It is observed from the figure that the histogram and pdf are in agreement. Similarly, Table 4.1 tabulates the mean, standard deviation and annual Sharpe ratio

Table 4.3 Mean and Standard Deviation of Annual Sharpe Ratios of the Four In-Sample Eigenportfolios

		EP1	EP2	EP3	EP4
$\mu_{\mu_{\boldsymbol{\theta}_k}}$	AR(1)	1.473	0	-0.32	0
	Data	1.598	-0.073	-0.24	-0.44
$\sigma_{\mu_{\boldsymbol{\theta}_k}}$	AR(1)	0.099	0	-0.021	0
	Data	0.108	0.098	0.299	0.265

Table 4.4 Mean and Standard Deviation of Annual Sharpe Ratios of the Four Out-Sample Eigenportfolios

		EP1	EP2	EP3	EP4
$\mu_{\mu_{\boldsymbol{\theta}_k}}$	AR(1)	1.65	0	-0.34	0
	Data	1.92	-0.06	-0.08	0.13
$\sigma_{\mu_{\boldsymbol{\theta}_k}}$	AR(1)	0.108	0	-0.022	0
	Data	0.118	0.339	0.448	0.261

values of eigenportfolio EOD returns obtained from market data measurements and their counterparts for AR(1) model as calculated from (4.16), (4.17), and (4.18), respectively. It is observed from the table that the model mimics measurements closely for this case where c is constant. However, eigenportfolio returns also show fat-tails, excessive kurtosis and asymmetry properties similar to asset returns. Normal distribution is used due to its simplicity. Figure 4.5a displays the profit and loss (PNL) curves of the first eigenportfolio generated from market data and AR(1) model. Similarly, Figure 4.5b displays PNL curves of the four eigenportfolios generated from market data. It is noted that the same eigenportfolio is used to calculate its in-sample EOD returns for the entire duration of $W = 600$ days. The Share ratio results with the out of sample EOD returns for measurement window $W = 200$ days ending on June 19, 2012 and 556 days of out of sample market data ending on September 5, 2014 are tabulated in Table 4.2. The results with the out of sample data has higher discrepancy between model and data than the results with in-sample data as expected.

Figure 4.7 displays normalized histogram for annual Sharpe ratio using EOD market returns of the first eigenportfolio (EP1) obtained from the empirical correlation matrix of four stocks {MMM, UTX, PFE, UNH}, $N = 4$, for the interval between January 24, 2014 and June 18, 2014 with the measurement window of $W = 600$ days. Normal pdf, with $\mu_{S_k}^m = 1.47$ and $\sigma_{S_k}^m = 0.09$ calculated from (4.24) and (4.25), respectively, that approximates the histogram is also displayed in this figure. It is noted that the parameter c is a random variable and modeled as $N\left(\mu_c = 1.73\, bps, \sigma_c^2 = 0.0001\, bps\right)$ in this case. Therefore, AR(1) model parameters for this market data are estimated as $\mu_c = 1.73$ bps, $\sigma_c^2 = 0.0001$ bps and $\rho = 0.77$. Figure 4.7 highlights the discrepancy between the means of these two distributions. Its main reason is the fact that market data is not mean stationary. The mean and variance of Sharpe ratio for the first eigenportfolio are calculated, from (4.24) and (4.25), respectively, as $\mu_{S_k}^m = 1.47$ and $\sigma_{S_k}^m = 0.09$. In contrast, they are measured

from market data as $\mu^d_{S_k} = 1.59$ and $\sigma^d_{S_k} = 0.108$. Similarly, Table 4.3 tabulates the mean and standard deviation of annual Sharpe ratios for the four eigenportfolio returns obtained from market data along with for AR(1) model as calculated from (4.24) and (4.25), respectively. Table 4.3 tabulates the mean and standard deviation of annual Sharpe ratios for the same experiment where the eigenportfolio returns are calculated using out of sample data. The results with the out of sample data has higher discrepancy between model and data than the results with in-sample data as expected.

This section validates the proposed framework to evaluate eigenportfolio returns. It utilizes AR(1) process as the statistical model for returns of assets in a basket to approximate market data due to its simplicity where the analysis is tractable.

4.5 Chapter Summary

Sharpe ratios for eigenportfolio returns of discrete AR(1) process are derived. The design of optimized super eigenportfolio (OSEP) is introduced. It is created by optimal allocation of investment capital among eigenportfolios based on maximization of Sharpe ratio. Eigenportfolio performance with respect to various parameters and metrics is investigated. It is showed through a four-stock investment basket that AR(1) approximation closely mimics its empirical correlation matrix obtained from market data. The proposed framework presents new insights for eigenportfolios and trading algorithms like statistical arbitrage that utilize them.

CHAPTER 5

SUBBAND PORTFOLIOS

In Chapter 4, performance analysis of eigenportfolios, that are generated through the eigendecomposition of empirical correlation matrix for asset returns for a basket, is given. In block transforms, the length of the basis functions is equal to the size of the input signal vector. Hence, transform and inverse transform matrices are square. Although this subspace structure provides simplicity to design transform and inverse transform matrices, it allows least possible mathematical freedom in tuning the orthonormal basis functions in the time and frequency domains for the desired requirements. KLT is the optimal orthonormal block transform that perfectly decorrelates the input signal in the subspace and maximally repacks its energy leading to dimensionality reduction [1].

In order to achieve more freedom for flexible subspace design, the length of the basis functions are extended in time. In general, if the arbitrary length for the basis sequences is allowed, filter bank or subband transform framework is utilized. Indeed, block transforms are interpreted as special filter banks [1]. The tradeoff is the fact that subband the transform matrix is rectangular and therefore, it is not invertible. The subband (filter bank) theory provides mathematical requirements to design invertible subband transform subspaces (filter banks) [1].

Low-pass quadrature mirror filter (QMF) is a filter where its magnitude response is the mirror image (around $\pi/2$) of another filter (high-pass) in a two-band filter bank. PR-QMF has perfect reconstruction properties imposed on these filters in a two-band filter bank structure. PR-QMF bank has been extensively used to split a signal spectrum into its various subbands (sub-spectra) in the frequency domain through subband tree structures [1].

In this chapter, optimal perfect reconstruction filter banks [15, 1, 14] to design subband portfolios are investigated. It is an extension of eigenportfolios. The goal is to exploit the freedom provided by longer basis sequences subband (vectors) than eigenvectors in order to design portfolios with various characteristics.

Similar to eigenportfolios, subband filter sequences (coefficients) of M-band optimal filter banks are used as capital allocation coefficients for M subband portfolios of $N-$asset basket where $M < N$. Sharpe ratios and market exposures of subband portfolios are calculated by using the framework developed in Chapter 4. They are compared with eigenportfolios for AR(1) signal model.

5.1 Optimal PR-QMF Design

For an N-asset basket, eigenanalysis of empirical correlation matrix for a predefined market history creates N eigenportfolios with their portfolio risks (volatility) and returns. The first eigenportfolio has the highest risk and full market exposure in a typical case. On the other hand, rest of the eigenportfolios may have lower risk levels and market exposures.

The main goal of generating subband subspace is to design a group of portfolios for the given empirical correlation matrix that have good performance. Therefore, self-hedged portfolios (less market exposure) with reasonable risk levels may be generated while preserving the desired properties like perfect decorrelation among subband portfolio returns.

Optimal PR-QMF banks are utilized to generate such subband portfolios [15, 1, 14]. The design details of PR-QMF banks are given in the following subsection.

5.1.1 Optimization Parameters for Optimal PR-QMF Design

An eigen subspace has the following properties,

1. Orthonormality.
2. Perfect reconstruction.

3. Energy compaction or gain of transform coding (GTC) over PCM maximization.
4. Perfect decorrelation of transform coefficients.

Eigendecomposition of $N \times N$ covariance (or correlation) matrix generates a $N \times N$ subspace that inherently satisfies these conditions. Another way of generating eigenvectors for a given covariance matrix is to solve the following optimization problem based on least squares [1]

$$\begin{aligned} \max \quad & \boldsymbol{\phi}_{\mathbf{k}}^{\mathbf{T}} \mathbf{C} \boldsymbol{\phi}_{\mathbf{k}} \\ \mathbf{s.t.} \quad & \boldsymbol{\phi}_{\mathbf{k}}^{\mathbf{T}} \boldsymbol{\phi}_{\mathbf{n}} = \delta_{k-n} \end{aligned} \tag{5.1}$$

where $\mathbf{C}$ is the covariance matrix, $\boldsymbol{\phi}_{\mathbf{k}}$ is the kth eigenvector, and δ_{k-n} is the Kronecker delta sequence. Optimal M-band PR-QMF bank with N-taps is designed by solving optimization problem given in (5.1) with additional constraints of desired features. The following performance metrics for the design optimal PR-QMFs were reported in the literature [15, 1, 14].

Orthonormal Perfect Reconstruction For M-bands PR-QMFs with N-taps, the orthonormal PR condition is defined as [15, 1, 14]

$$\sum_{n} h_i(n)\, h_j(n - kM) = \delta_k \delta_{i-j} \tag{5.2}$$

where filter lengths are integer multiples of the number of bands in PR-QMF bank.

Energy Compaction For paraunitary transformation, the Parseval theorem states the energy preservation constraint [1, 14]

$$\sigma_x^2 = \frac{1}{2}\left(\sigma_L^2 + \sigma_H^2\right) \tag{5.3}$$

where σ_x^2 is the variance of zero-mean input with correlation matrix $\mathbf{R}$. σ_L^2 and σ_H^2 are variances of the low-pass and high-pass filter outputs, respectively. They can also be calculated as

$$\begin{aligned} \sigma_L^2 &= \mathbf{h_L^T R h_L} \\ \sigma_H^2 &= \mathbf{h_H^T R h_H} \end{aligned} \tag{5.4}$$

where $\mathbf{h_L}$ and $\mathbf{h_H}$ is the low-pass and high-pass filters in vector form, respectively. Once the low-pass filter is generated, its mirror high-pass filter is obtained as

$$h_H(n) = (-1)^n h_L(n) \tag{5.5}$$

The energy compaction metric is [1]

$$G_{TC} = \frac{\sigma_x^2}{\left(\sigma_L^2 \sigma_H^2\right)^{1/2}} \tag{5.6}$$

It is clear from (5.6) that the maximization of σ_L^2 in (5.4) is sufficient condition for energy compaction [1].

Correlation Between Subband Signals Let $\mathbf{A}_{SB}$ be a matrix that PR-QMFs are placed as column-wise. Then, p is defined as [1]

$$p = \sum_{i=1}^{N-1} \sum_{j=1, i \neq j}^{N-1} |R_\theta(i,j)| \tag{5.7}$$

where

$$\mathbf{R}_\theta = \mathbf{A^T}_{SB} \mathbf{R} \mathbf{A}_{SB} \tag{5.8}$$

For perfect decorrelation condition, $p = 0$.

Zero-Mean Most energy of real world signals like image frames is concentrated around the DC frequency. Practical signal decomposition techniques are expected to be able to represent the DC component by only one basis function of the orthonormal set. Therefore, except low-pass filter, all filters of the subband filter bank should have zero-mean [15, 1, 14],

$$\sum_{n=1}^{N-1} h\left(n\right) = 0 \tag{5.9}$$

This requirement implies that there should be at least one zero of the low-pass filter $H\left(e^{j\omega}\right)$ at $\omega = \pi$. From investment portfolio design point of view, it means zero market exposure condition for a basket of assets with similar correlation to the overall market.

Energy Compaction The optimization problem to generate optimal PR-QMFs that maximizes the energy compaction with the constraints is defined as [15, 1, 14];

$$\begin{aligned} \max \quad & \mathbf{h_i^T R h_i} \\ \mathbf{s.t.} \quad & \sum_n h_i\left(n\right) h_j\left(n - kM\right) = \delta_k \delta_{i-j} \\ & p = 0 \\ & \sum_{n=1}^{N-1} h_i\left(n\right) = 0 \\ & \sum_{n=1}^{N-1} \left(-1\right)^n h_i\left(n\right) = 0 \end{aligned} \tag{5.10}$$

Note that zero-mean condition for low-pass filter is not included.

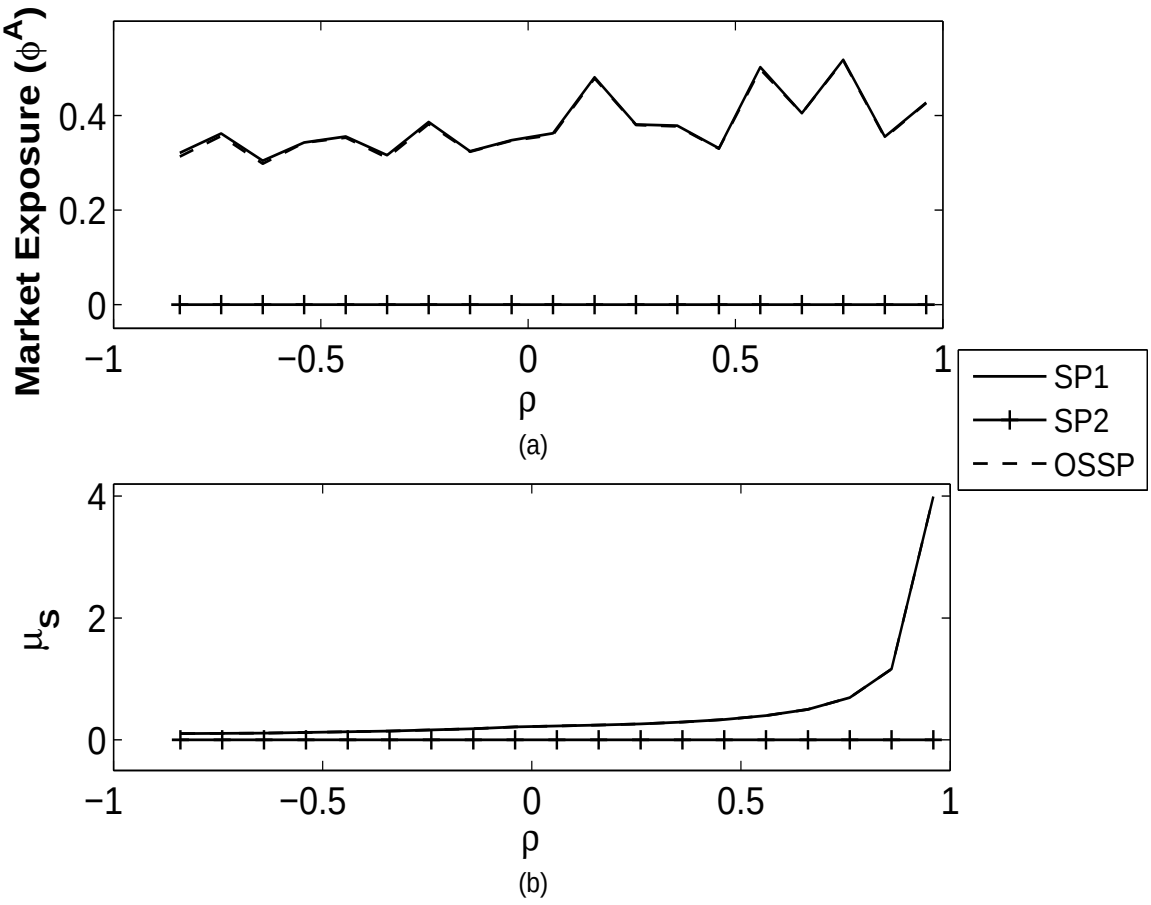

Figure 5.1 (a) Market exposures, $\boldsymbol{\phi}^A$, and (b) expected values of Sharpe ratios, μ_S, for the subband portfolios (SPs) of AR(1) process generated by optimal $M = 2$ band perfect reconstruction filter bank with zero-mean constraint along with optimized super subband portfolio (OSSP) for $\mu_c = 1$ bps, $N = 30$, and with respect to ρ.

5.2 Performance of Subband Portfolios for AR(1) Process

Sharpe ratio and market exposure of subband portfolios for AR(1) random vector process are calculated using Equations (4.24) and (4.19) derived in Chapter 4, respectively. Their performances are evaluated and compared with the eigenportfolios. Moreover, the empirical correlation matrix for a basket of four stocks is measured from market data and approximated by an AR(1) process to validate the proposed framework.

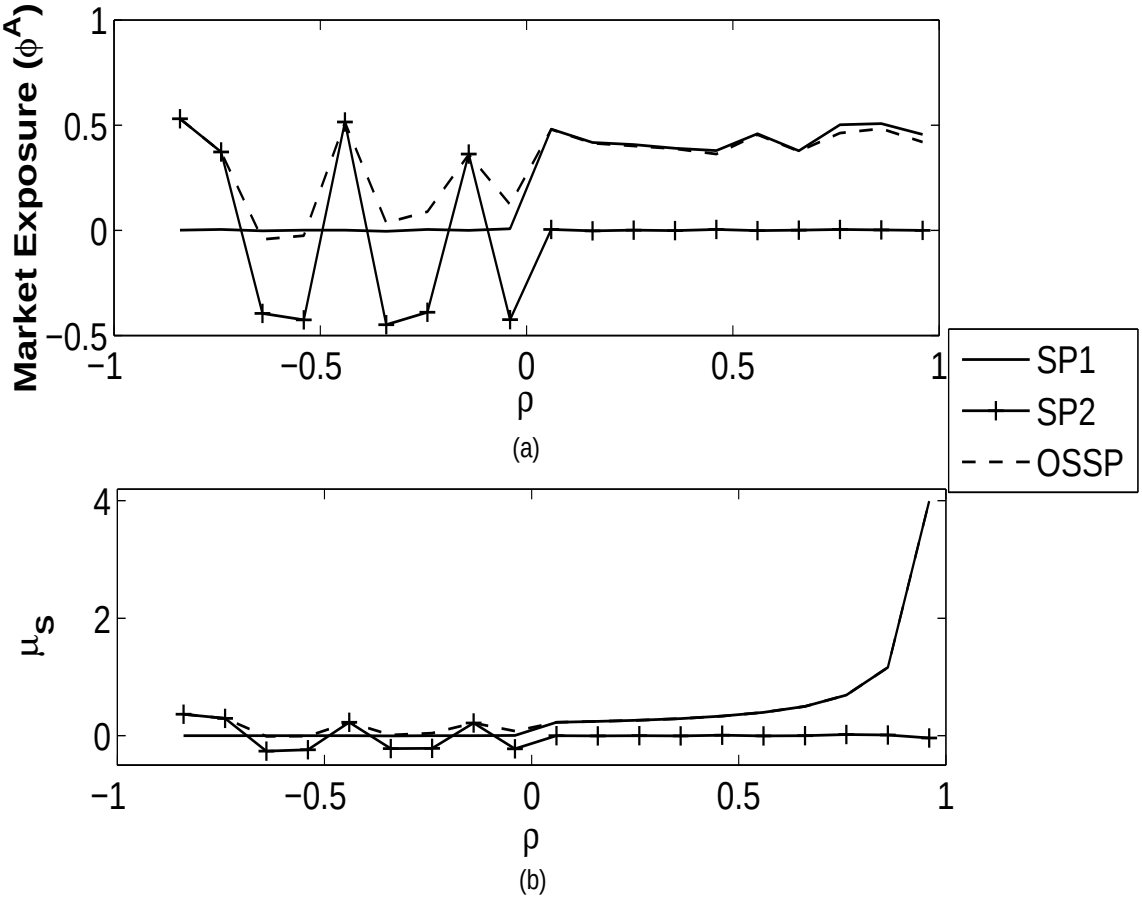

Figure 5.2 (a) Market exposures, $\boldsymbol{\phi}^A$, and (b) expected values of Sharpe ratios, μ_S, for the subband portfolios (SPs) of AR(1) process generated by optimal $M = 2$ band perfect reconstruction filter bank along with optimized super subband portfolio (OSSP) for $\mu_c = 1$ bps, $N = 30$, and with respect to ρ.

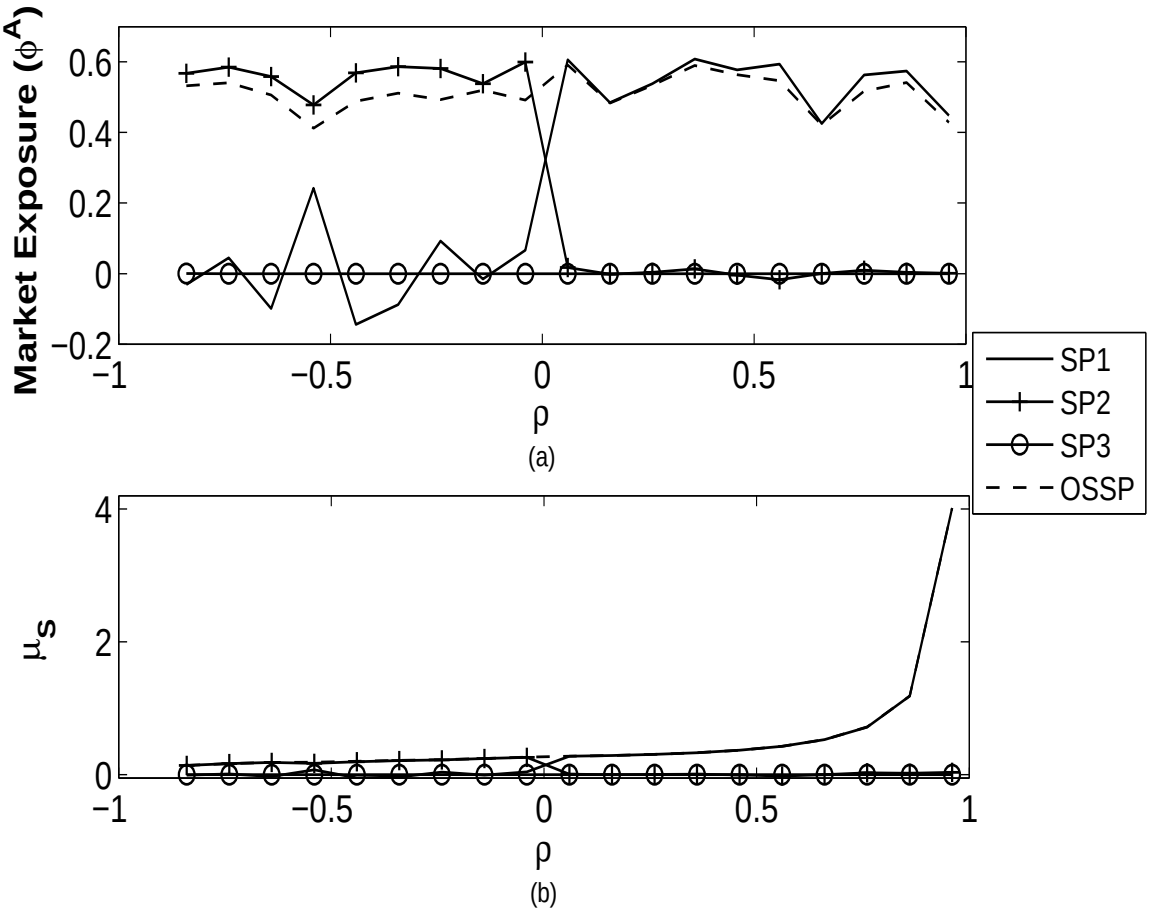

Figure 5.3 (a) Market exposures, $\boldsymbol{\phi}^A$, and (b) expected values of Sharpe ratios, μ_S, for the subband portfolios (SPs) of AR(1) process generated by optimal $M = 3$ band perfect reconstruction filter bank with zero-mean constraint along with optimized super subband portfolio (OSSP) for $\mu_c = 1$ bps, $N = 30$, and with respect to ρ.

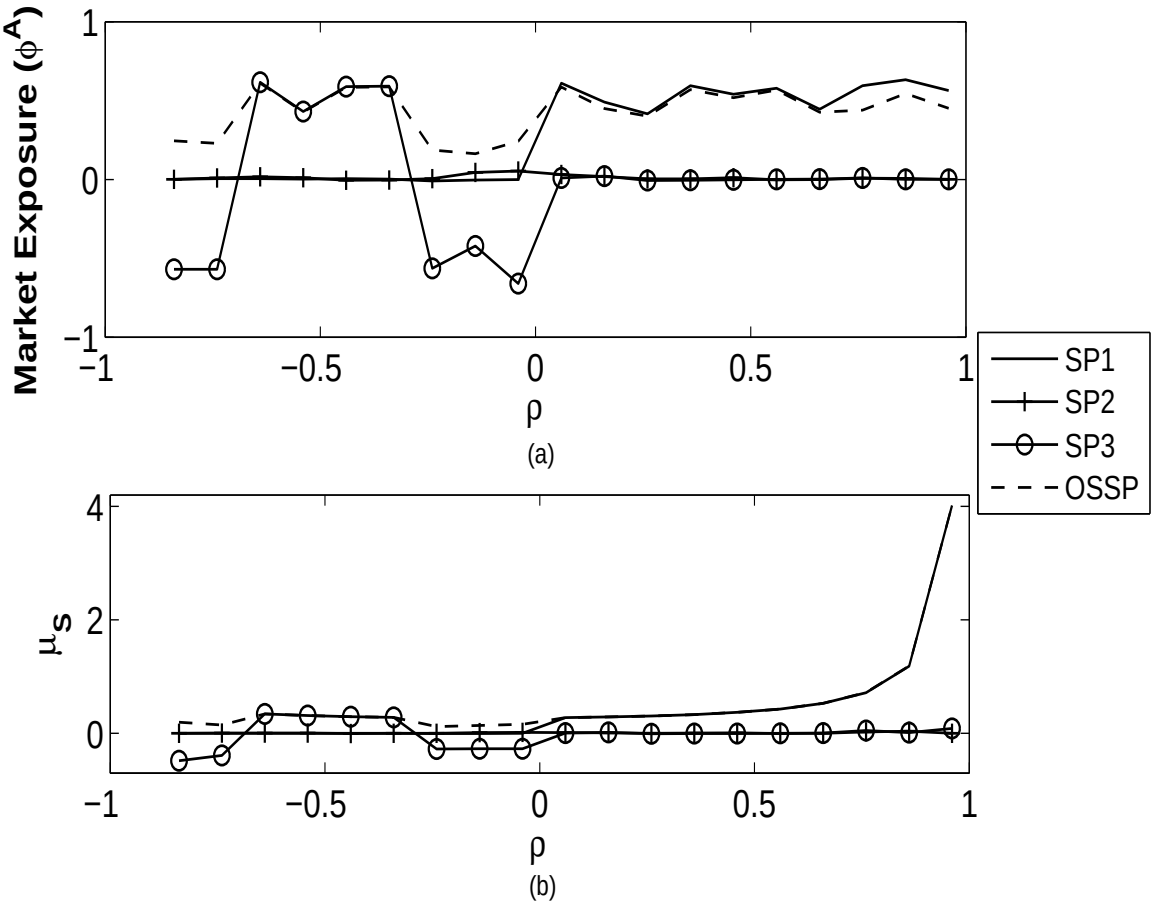

Figure 5.4 (a) Market exposures, $\boldsymbol{\phi}^A$, and (b) expected values of Sharpe ratios, μ_S, for the subband portfolios (SPs) of AR(1) process generated by optimal $M = 3$ band perfect reconstruction filter bank along with optimized super subband portfolio (OSSP) for $\mu_c = 1$ bps, $N = 30$, and with respect to ρ.

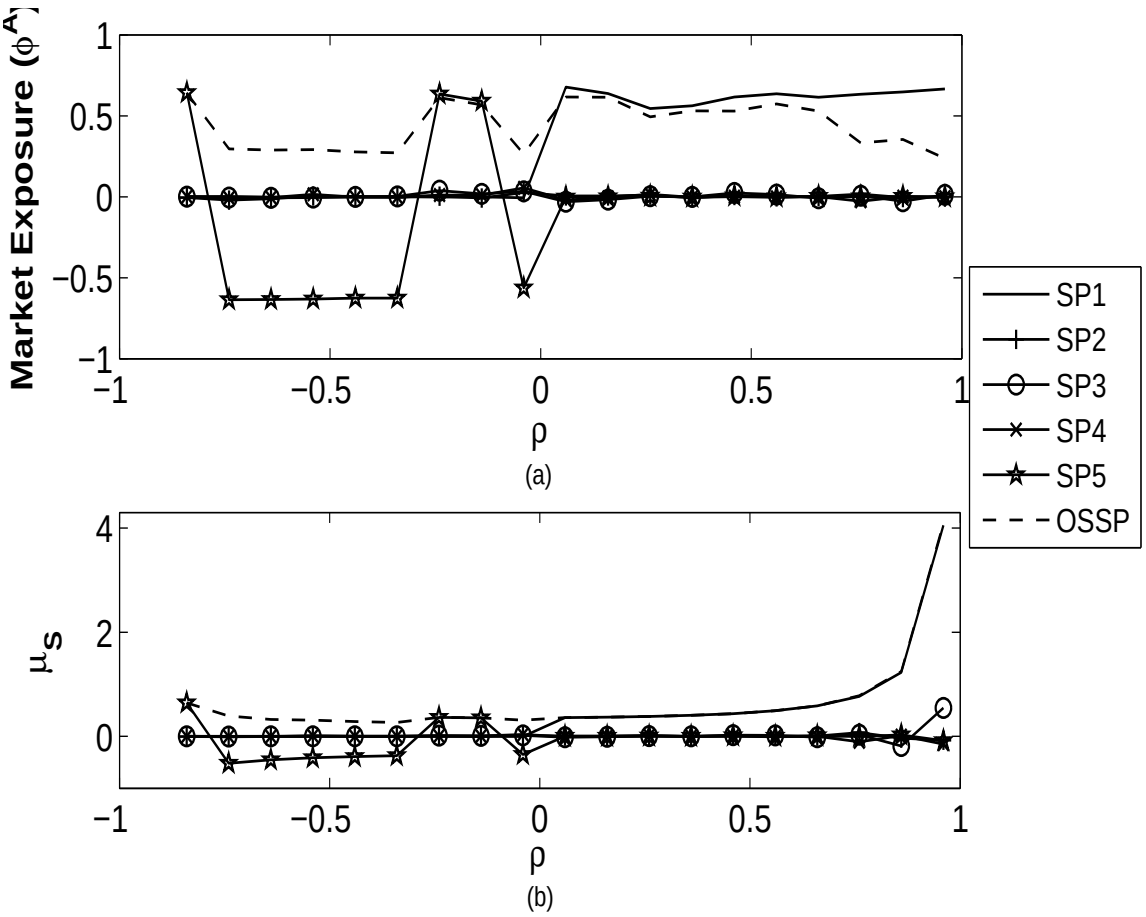

Figure 5.5 (a) Market exposures, $\boldsymbol{\phi}^A$, and (b) expected values of Sharpe ratios, μ_S, for the subband portfolios (SPs) of AR(1) process generated by optimal $M = 5$ band perfect reconstruction filter bank along with optimized super subband portfolio (OSSP) for $\mu_c = 1$ bps, $N = 30$, and with respect to ρ.

5.2.1 Subband Portfolios of AR(1) Process

The market exposures, ϕ^A, and expected values of Sharpe ratios, μ_S, for $M = 2$ bands and $N = 30$ taps (portfolio size) subband portfolios of AR(1) process, with $\mu_c = 1$ bps, as a function of ρ are displayed in Figure 5.1a and 5.1b, respectively. ϕ^A and μ_S of optimized super subband portfolio (OSSP) that is generated using (4.46) is also included in these figures. Same simulation parameters set for eigenportfolios in Section 4.4.1 are also used for performance comparisons. Figure 5.2a and 5.2b display the market exposures, ϕ^A, and expected values of Sharpe ratios for the same scenario without zero-mean condition. A similar simulation with $M = 3$ and $M = 5$ with and without zero-mean condition are displayed in Figure 5.3a, 5.3b 5.4a, 5.4b, 5.5a, 5.5b, respectively.

Figures for expected values of Sharpe ratios display that OSSP has the best performance among subband portfolios. SP1 has the highest market exposure as expected. Performance of the other subband portfolios depend on whether zero-mean condition is enforced or not. When zero-mean condition is not included in the optimization, they have small market exposure and lower value for expected Sharpe ratio.

The market exposures, ϕ^A, and expected values of Sharpe ratios, μ_S, for the odd indexed eigenportfolios of AR(1) process with same simulation parameters are displayed in Figure 4.1a and 4.1b, respectively. Similarly, Figure 4.2a and 4.2b display the ϕ^A and μ_S of the even indexed eigenportfolios, respectively. When subband portfolios are compared with eigenportfolios of AR(1) random vector process, it is observed that eigenportfolios deliver slightly better Sharpe ratio. On the other hand, market exposure of eigenportfolios are higher than subband portfolios. In particular, EP1 has full market exposure and the highest risk. Subband portfolios offer significantly less market exposure than eigenportfolios. SP1 has $40\% - 50\%$ market exposure and delivers smaller levels of risk compared to EP1.

Table 5.1 Mean, Standard Deviation and Annual Sharpe Ratios of End of Day (EOD) Returns for In-Sample Subband Portfolios

		SP1	EP1	SP2	EP2	EP3	EP4
$\mu_{\boldsymbol{\theta}_k}$(bps)	AR(1)	0.081	0.081	0.0	0.0	-0.005	0.00
	Data	0.081	0.082	0.001	-0.002	-0.012	-0.003
$\sigma_{\boldsymbol{\theta}_k}$(bps)	AR(1)	1.16	1.06	0.44	0.54	0.32	0.27
	Data	1.03	0.98	0.007	0.66	0.48	0.37
S_k (annual)	AR(1)	1.11	1.122	0.0	0.00	-0.251	0.00
	Data	1.25	1.328	0.032	-0.068	-0.411	-0.14

5.2.2 Subband Portfolios of a Basket

A basket of four stocks {MMM, UTX, PFE, UNH} is created to validate the proposed framework to design subband portfolios. End of day (EOD) returns are used in this study. The empirical correlation matrix for the measurement window of $W = 600$ days ending on January 24, 2014, is calculated and optimization problem in (5.10) is solved. Note that only $M = 2$ band PR-QMF bank can be generated due to PR conditions. Large window sizes resulted in comparable values for mean and variance of asset returns, and a good AR(1) approximation to market data with W=600 is obtained for that basket. One dollar investment in each subband portfolio and no transaction cost are considered. It is noted that in-sample measurements are utilized in this experiment.

Table 5.1 tabulates the mean, standard deviation and annual Sharpe ratio values for two subband portfolios and four eigenportfolios of the EOD returns generated from the empirical correlation matrix, $W = 600$, of four-stock basket {MMM, UTX, PFE, UNH} for the market data ending on January 24, 2014 and their counterparts for AR(1) model as calculated from (4.16), (4.17), and (4.18), respectively. It is observed from the table that the model mimics measurements closely for this case where c is

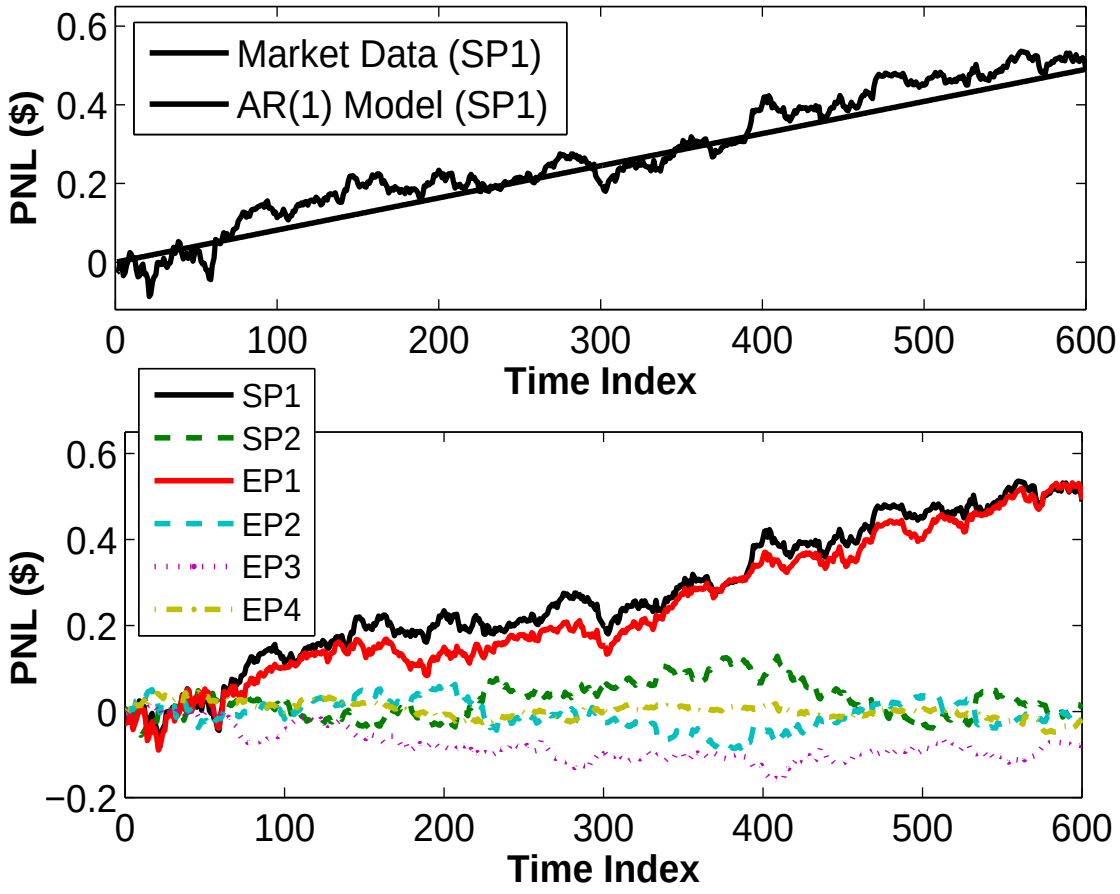

Figure 5.6 Profit and Loss (PNL) curves of end of day (EOD) returns for (a) the first subband portfolio, and (b) the two subband portfolios, generated from empirical correlation matrix of the basket {MMM, UTX, PFE, UNH}, $N = 4$ with $W = 600$ days ending on January 24, 2014. The linear PNL curve generated for the first eigenportfolio of AR(1) process per (4.16) and for the parameters $c = 0.02$ bps and $\rho = 0.75$ is also displayed in (a) to highlight the model fit.

Table 5.2 Mean, Standard Deviation and Annual Sharpe Ratios of End of Day (EOD) Returns for Out-Sample Subband Portfolios

		SP1	EP1	SP2	EP2	EP3	EP4
$\mu_{\boldsymbol{\theta}_k}$(bps)	AR(1)	0.074	0.074	0.0	0.0	-0.003	0.00
	Data	0.065	0.072	-0.012	-0.003	-0.0	-0.012
$\sigma_{\boldsymbol{\theta}_k}$(bps)	AR(1)	0.89	0.93	0.70	0.4	0.23	0.19
	Data	0.99	0.75	0.31	0.62	0.54	0.34
S_k (annual)	AR(1)	1.18	1.27	0.0	0.00	-0.23	0.00
	Data	1.16	1.54	-0.27	-0.085	-0.007	-0.57

Table 5.3 Mean and Standard Deviation of Annual Sharpe Ratios of the In-Sample Subband and Eigen Portfolios

		SP1	EP1	SP2	EP2	EP3	EP4
$\mu_{\mu_{\boldsymbol{\theta}_k}}$	AR(1)	0.86	1.473	0.0	0	-0.32	0
	Data	1.511	1.598	0.6	-0.073	-0.24	-0.44
$\sigma_{\mu_{\boldsymbol{\theta}_k}}$	AR(1)	0.04	0.099	0.0	0	-0.021	0
	Data	0.08	0.108	0.04	0.098	0.299	0.265

Table 5.4 Mean and Standard Deviation of Annual Sharpe Ratios of the Out-Sample Subband and Eigen Portfolios

		SP1	EP1	SP2	EP2	EP3	EP4
$\mu_{\mu_{\boldsymbol{\theta}_k}}$	AR(1)	0.93	1.65	0.0	0.0	-0.34	0.0
	Data	1.90	1.92	0.15	-0.06	-0.08	0.13
$\sigma_{\mu_{\boldsymbol{\theta}_k}}$	AR(1)	0.06	0.108	0.0	0.0	-0.022	0.0
	Data	0.14	0.118	0.19	0.339	0.448	0.261

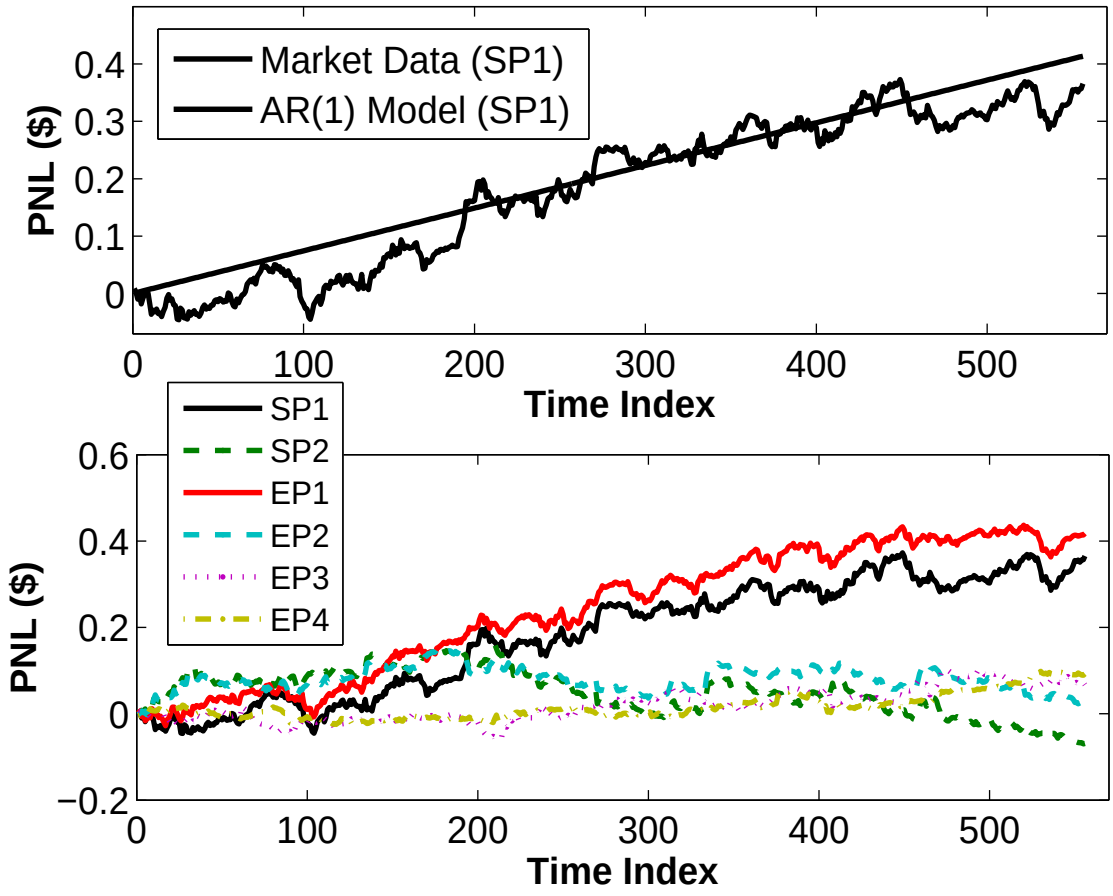

Figure 5.7 (a) Profit and Loss (PNL) curves of end of day (EOD) returns for the out-sample first subband portfolio generated from empirical correlation matrix of the basket {MMM, UTX, PFE, UNH}, $N = 4$, with $W = 200$ days ending on June 19, 2012 and 556 days out of sample market data ending on September 5, 2014. The linear PNL curve generated for the first subband portfolio of AR(1) process per (4.16) and for the parameters $c = 0.013$ bps and $\rho = 0.81$ is also displayed to highlight the model fit. (b) Profit and Loss (PNL) curves of end of day (EOD) returns for all subband and eigen portfolios.

constant. Figure 5.6a displays PNL curves of the first subband portfolio generated from market data and AR(1) model. Similarly, Figure 5.6b displays PNL curves of the two subband and four eigen portfolios generated from market data. It is noted that the same eigenportfolio is used to calculate its in-sample EOD returns for the entire duration of $W = 600$ days. The Share ratio results with the out of sample EOD returns for measurement window $W = 200$ days ending on June 19, 2012 and 556 days of out of sample market data ending on September 5, 2014 are tabulated in Table 5.2. The results with the out of sample data has higher discrepancy between model and data than the results with in-sample data as expected.

Table 5.3 tabulates the mean and standard deviation of annual Sharpe ratios of the two in-sample two subband and four eigen portfolios created for the empirical correlation matrix of the basket {MMM, UTX, PFE, UNH}, $N = 4$, with the measurement window $W = 600$ days of market data for the interval between January 24, 2014 and June 18, 2014. The AR(1) model parameters of (2.1) are estimated from market data as $\mu_c = 1.73$ bps and $\rho = 0.77$. There is a the discrepancy between the model and the data. Its main reason is the fact that market data is not mean stationary. The mean and standard deviation of annual Sharpe ratios of same experiment with out of sample EOD returns for measurement window W = 200 days ending on June 19, 2012 and 400 days of out of sample market data tabulated in Table 5.4.

5.3 Chapter Summary

In this chapter, subband portfolios generated by using the theory of optimal PR-QMF banks are introduced. Their Sharpe ratio and market exposure performance are evaluated and compared with eigenportfolios for AR(1) signal model. The performance results show that subband portfolios offer less market exposure (less risk) with slightly less expected Sharpe ratio.

CHAPTER 6

QUANTIZATION OF SUBSPACES FOR SPARSE REPRESENTATION

KLT has been employed in multivariate data processing and dimension reduction although the application specific interpretation of principal components (eigenvectors) is often difficult in some cases [13, 42, 49, 20]. Moreover, small but non-zero loadings (elements) of each principal component (PC) (or eigenvector) bring implementation cost that is hard to justify in applications such as generation and maintenance (rebalancing) of eigen portfolios in finance [20, 41, 2]. This and other applications that utilize loading coefficients have motivated researchers to study sparsity of PCs in eigen analysis of matrices. Furthermore, unevenness of signal energy distributed among PCs in eigen subspace is reflected in eigenvalues (coefficient variances) that lead to dimension reduction. The latter is the very foundation of transform coding successfully used in visual signal processing and data compression [1, 26, 17]. Therefore, both dimension reduction and sparsity of basis functions (vectors) are significant attributes of orthogonal transforms widely utilized in many applications. This recent development has paved the way for our study where a rate-distortion based framework to sparse basis functions of subspaces including eigen subspace of a given covariance matrix is proposed. The challenge is to maximize explained variance by minimum number of PCs, also called energy compaction [1], while replacing the less significant samples (loading coefficients) of basis functions with zero to achieve the desired level of sparsity in signal representation.

Regularization methods have been used to make an ill-conditioned matrix invertible or to prevent overfitting [7, 22]. It is achieved by adding an ℓ_1 (norm-1) or ℓ_2 constraint in the optimization. As an example, ridge regression exploits an ℓ_2 penalty for stabilization in the least squares problem [7]. Eigenfiltering is another

popular method employed for regularization [7, 22]. More recently, regularization methods have been also utilized for sparsity. ℓ_0 regularizer leads to a sparse solution. On the other hand, it makes the optimization problem non-convex.

ℓ_1 regularizer, so called lasso, is a widely used approximation (convex relaxation) to ℓ_0 case [42, 38]. Another ℓ_1 based method was proposed in [11] for sparse portfolios. SCoTLASS [42] and SPCA [49] utilize the ℓ_1 and ℓ_2 regularizers for sparse approximation to principal components (PCs), respectively. The sparse PCA is modeled in [42, 49] as an explained variance maximization problem where number of non-zero elements in the PCs considered as a basis design constraint. These methods suffer from potentially being stuck in local minima due to the non-convex nature of the optimization. A convex relaxation method called SDP Relaxations for Sparse PCA (DSPCA) using semidefinite programming (SDP) was proposed to deal with a simpler optimization [20]. Empirical performance results for certain cases indicate that DSPCA may generate sparse PCs that preserve slightly more explained variance than SCoTLASS [42] and SPCA [49] for the same sparsity level. A nonnegative variant of the sparse PCA problem that forces the elements of each principal components (PCs) to be nonnegative, is introduced in [47]. Nonnegative sparse PCA (NSPCA) offers competitive performance to SCoTLASS, SPCA and DSPCA in terms of explained variance for a given sparsity. However, sign of the PC elements bear specific information for the applications of interests such as eigenportfolios. Thus, NSPCA is not applicable for all types of applications. Another lasso based approach, so called sparse PCA via regularized SVD (sPCA-rSVD), is proposed in [37]. Simulation results for certain cases show that sPCA-rSVD provides competitive results to SPCA. A variation of sPCA-rSVD, so called sparse principal components (SPC), that utilizes the penalized matrix decomposition (PMD) is proposed in [45]. PMD that computes the rank K approximation of a given matrix is proposed in [45]. It utilizes the lasso penalty for sparsity. Unfortunately, none of these methods result

in guaranteed sparsity regardless of their prohibitive computational cost for high dimensions. Moreover, the lack of mathematical framework to measure distortion, or explained variance loss, for a desired sparsity level makes sparse PCA methods of this kind quite ad-hoc and difficult to use. On the other hand, the simple (hard) thresholding technique is easy to implement [13]. It performs better than SCoTLASS and slightly worse than SPCA [49]. Although simple thresholding is easy to implement, it may cause unexpected distortion levels as called variance loss. Soft thresholding (ST) is another technique that is utilized for sparse representation in [49]. Certain experiments show that ST offers slightly better performance than simple thresholding [49]. Therefore, threshold selection plays a central role in sparsity performance.

In this chapter, a subspace sparsing framework based on the rate-distortion theory [1, 33, 29, 6] is proposed. It may be considered as an extension of the simple or soft thresholding method to unify sparse representation problem with an optimal quantization method widely used in the source coding field [1, 13, 26, 17, 6]. The method employs a varying size mid-tread (zero-zone) pdf-optimized (Lloyd-Max) quantizer designed for component histogram of each eigenvector (or the entire eigen matrix) to achieve the desired level of distortion (sparsity) in the subspace with reduced cardinality [33, 29, 24]. Although eigen subspace is focused in this chapter, the proposed method is applicable to sparse any subspace. There are studies in the literature that jointly examine compressed sensing (CS) and quantization [9], this is the first attempt to utilize pdf-optimized quantization based methods for sparse PCA problem. Eigen subspace of autoregressive order one, AR(1), discrete process is focused due to the availability of closed form expressions for its eigenvectors and eigenvalues. It is known that AR(1) process approximates well many real world signals [1]. Eigenportfolios of NASDAQ-100 index is also sparsed by using this method. It is noted that the proposed method to sparse a subspace through quantization

of its basis functions is a marked departure from the traditional transform coding where transform coefficients, in the subspace, are quantized for dimension reduction also called zonal sampling in the literature [1, 26, 17]. Therefore, the trade-off between subspace orthogonality and sparsity is investigated from the rate-distortion perspective for the case where original values of transform coefficients are employed. Then, a comparative performance of the proposed method is provided along with the various methods reported in the literature such as ST [49], SPCA [49], DSPCA [20], and SPC [45] with respect to the metrics of non-sparsity (NS) and variance loss (VL).

6.1 Subspace Quantization

In transform coding (TC), sparsity in transform coefficients is desired. In contrast, any sparse transform including KLT aims to sparse subspace (transform matrix) where values of basis vector components are important and interpreted as loading coefficients in some applications [34, 31, 8, 39, 16, 40]. Quantization of a given subspace with an optimally designed single quantizer Q, or a set of quantizers $\{Q_k\}$ in the case of quantizing each basis function (vector) independently, is defined as

$$\widehat{\Phi} = Q(\Phi) \tag{6.1}$$

In this case, Q is a pdf-optimized midtread quantizer designed for the entire transform matrix. Then, transform coefficients are obtained by using the quantized matrix

$$\hat{\boldsymbol{\theta}} = \widehat{\Phi}\mathbf{x} \tag{6.2}$$

Unlike in transform coding (TC), coefficients are not quantized in sparse representation methods unless desired for the given application. Instead, coefficients of the projection onto quantized subspace for a given signal vector are obtained. As in TC,

quantization error equals to reconstruction error, both in mse, when the signal is reconstructed as (2.22). Mean squared quantization error due to sparsity of subspace is expressed as

$$\sigma_{q,S}^2 = \frac{1}{N^2} \sum_{k=0}^{N-1} \widetilde{\boldsymbol{\phi}_k}^{\mathbf{T}} \widetilde{\boldsymbol{\phi}_k} \tag{6.3}$$

where $\widetilde{\boldsymbol{\phi}_k} = \boldsymbol{\phi}_k - \widehat{\boldsymbol{\phi}_k}$.

6.2 Quantization of Eigen Subspace for AR(1) Process

In this section, modelling probability density function (pdf) (or histogram) of eigenvector components (PC loadings) for the Toeplitz correlation matrix of AR(1) source expressed in (2.20) is investigated. A pdf-optimized zero-zone quantizer is designed for each eigenvector that is being sparsed. One might also use a single quantizer for the entire eigen matrix in order to reduce implementation cost. Rate-distortion performance of such quantizers is evaluated. Performance comparisons of the proposed sparse KLT (SKLT) method with ST [49], SPCA [49], DSPCA [20], and SPC [45] methods is presented in terms of non-sparsity (NS) and variance loss (VL) metrics in the following section.

6.2.1 Probability Density Functions (pdf) of Eigenvector Components

Arcsine Distribution of Continuous Sinusoidal Function In this section, the probability density of eigenvector components is modeled in order to design pdf-optimized quantizers to sparse them. Each eigenvector of AR(1) process is generated by a sinusoidal function as expressed in (2.20). Probability density function (pdf), with arbitrary support, of a continuous sinusoidal function is modeled as [25, 5]

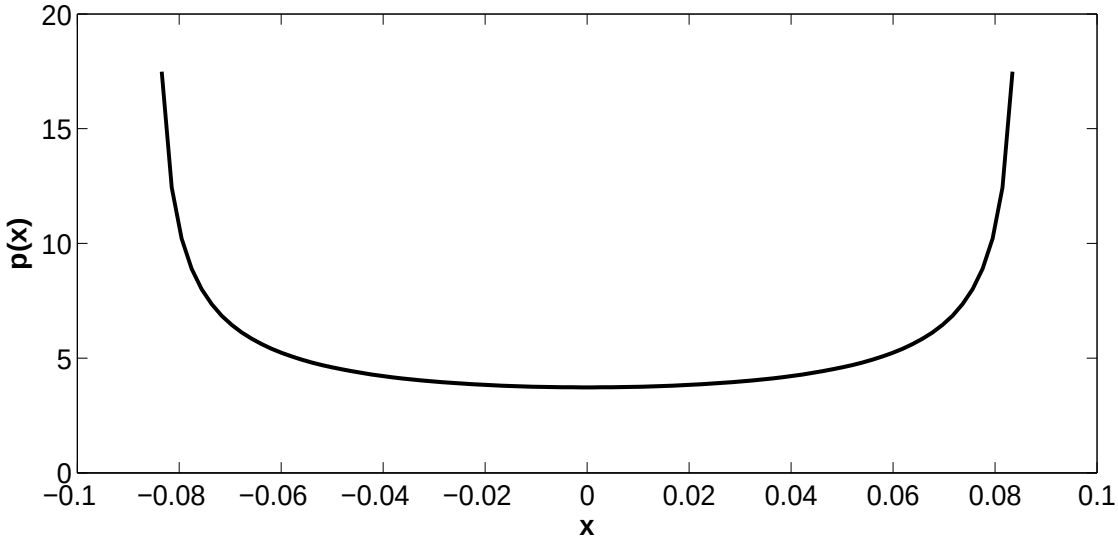

Figure 6.1 Probability density function of arcsine distribution for $a = -0.0854$ and $b = 0.0854$. Loadings of second PC for AR(1) signal source with $\rho = 0.9$ and $N = 256$ are fitted to arcsine distribution by finding minimum and maximum values in the PC.

$$p\left(x\right) = \frac{1}{\pi\sqrt{\left(x-a\right)\left(b-x\right)}} \tag{6.4}$$

where a and b define the support, $a \leq x \leq b$. Cumulative distribution function (cdf) of such a function type is of arcsine distribution and expressed as

$$P(x) = \frac{2}{\pi}\arcsin\left(\sqrt{\frac{x-a}{b-a}}\right) \tag{6.5}$$

Mean and variance of the arcsine distribution are calculated as

$$\mu = \frac{a+b}{2} \tag{6.6}$$

$$\sigma^2 = \frac{\left(b-a\right)^2}{8} \tag{6.7}$$

The pdf of arcsine distribution is symmetric and U-shaped. Figure 6.1 shows the pdf of arcsine distribution with parameters $a = -0.0854$ and $b = 0.0854$. Log-concavity of a pdf $p(x)$ is the sufficient condition for the uniqueness of a pdf-optimized quantizer. However, arcsine distribution type has the log-convex property [4]. It is stated in [46] that for exponential sources and the sources with strictly log-convex pdfs, the quantizer intervals (bins) and their bin representation (quanta) values are globally optimum and unique. Therefore, pdf-optimized quantizers can be designed for arcsine distribution [33, 29]. Second principal component, $\boldsymbol{\phi}_1$, of AR(1) source for $\rho = 0.9$ and size of $N = 256$ is shown to be fit by arcsine distribution with $a = \min(\boldsymbol{\phi}_1) = -0.0854$ and $b = \max(\boldsymbol{\phi}_1) = 0.0854$, respectively. Minimum and maximum valued components of the k^{th} eigenvector depend on ρ, ω_k and N as stated in (2.20). In order to maintain equal distortion levels among quantizers to sparse eigenvectors, optimal intervals are calculated for zero-zones of pdf-optimized midtread quantizers. Thus, most of the small valued eigenvector components are likely to be quantized as zero.

Eigenvector Component Histograms for AR(1) Process Figure 6.2a and 6.2b display the normalized histograms of the first and second eigenvector components (PC1 and PC2 loading coefficients) for AR(1) process with $\rho = 0.9$ and $N = 1,024$. The value of N is selected large enough to generate proper histograms. The intervals of the histograms, Δ_k, are set as $\Delta_k = \frac{\max(\boldsymbol{\phi}_k) - \min(\boldsymbol{\phi}_k)}{N}$ where $\boldsymbol{\phi}_k$ is k^{th} eigenvector. The dashed lines in each normalized histogram show the probability that is calculated by integrating the pdf of arcsine distribution in (6.4) for each bin interval. The histogram displayed in Figure 6.2a has only one side of the arcsine pdf as expected from (2.20). In contrast, Figure 6.2b displays the histogram with complete arcsine pdf shape. These figures confirm arcsine distribution type for eigenvector components of an AR(1) process.

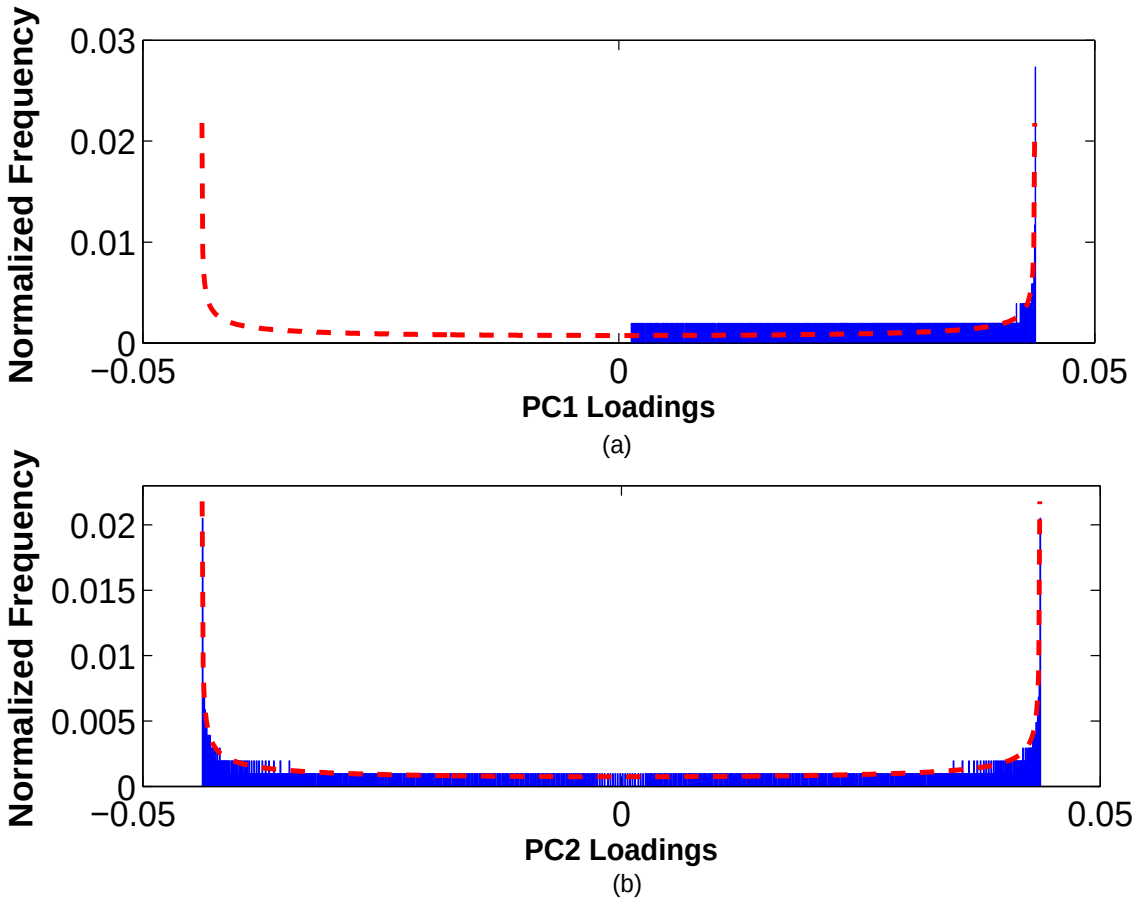

Figure 6.2 Normalized histograms of (a) PC1 and (b) PC2 loadings for AR(1) signal source with $\rho = 0.9$ and $N = 1,024$. The dashed lines in each histogram show the probability that is calculated by integrating arcsine pdf for each bin interval.

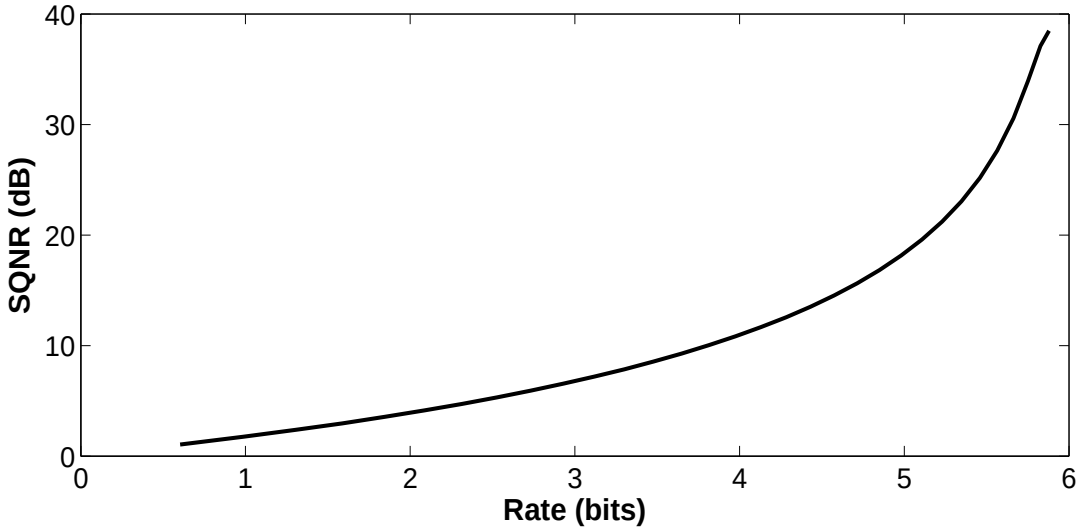

Figure 6.3 Rate (bits)-distortion (SQNR) performance of zero mean and unit variance arcsine pdf-optimized quantizer for $L = 65$ bins. Distortion level is increased by combining multiple bins around zero in a larger zero-zone.

6.2.2 Rate-Distortion Performance of Arcsine pdf-Optimized Zero-Zone Quantizer

In this section, the rate-distortion performance of arcsine pdf-optimized zero-zone quantizer is investigated. Rate of quantizer output is calculated by using first order entropy as defined in (2.31). Distortion caused by the quantizer is calculated in mse and represented in SQNR as defined in (2.29). Figure 6.3 displays rate-distortion performance of such a quantizer with $L = 65$. It is observed that the performance of such a quantizer does not improve significantly for $L > 65$. Therefore, as a design step, $L = 65$ is used for the baseline quantizer where original zero-zone was widened by combining the adjacent bins. Hence, distortion level is increased by increasing the zero-zone of the quantizer for more sparsity where rate decreases, accordingly. One may design a midtread quantizer with zero-zone for each eigenvector (PC) or for the entire eigen matrix to achieve the desired level of matrix (subspace) sparsity [33, 29].

Table 6.1 Relevant Parameters of SKLT Method for the First Eleven PCs of AR(1) Source

	ω	λ	a	b	σ^2	R	L_k	S_k
PC1	0.0114	18.77	-0.0853	0.0853	0.0036	5.6546	51	26
PC2	0.0229	18.14	-0.0853	0.0853	0.0036	5.6563	51	28
PC3	0.0344	17.17	-0.0856	0.0856	0.0037	5.6588	51	40
PC4	0.0459	15.97	-0.0857	0.0857	0.0037	5.6620	51	34
PC5	0.0575	14.64	-0.0860	0.0860	0.0037	5.6655	51	36
PC6	0.0691	13.29	-0.0862	0.0862	0.0037	5.6691	51	38
PC7	0.0808	11.97	-0.0864	0.0864	0.0037	5.6725	51	42
PC8	0.0925	10.73	-0.0866	0.0866	0.0037	5.6754	51	42
PC9	0.1043	9.60	-0.0868	0.0868	0.0038	5.6790	51	40
PC10	0.1162	8.58	-0.0869	0.0869	0.0038	5.6819	51	36
PC11	0.1281	7.67	-0.0871	0.0870	0.0038	5.6835	51	44

6.2.3 A Simple Method for Sparse KLT

In this section, the proposed method to sparse eigen subspace of AR(1) process is explained through a design example. The values of relevant parameters for the example are tabulated in Table 6.1.

The steps of design are summarized as follows.

1. First order correlation coefficient ρ is calculated from available data set as described in (2.2). Assume that $\rho = 0.9$ for the given example with $N = 256$.

2. Correlation matrix $\mathbf{R_x}$ for the measured ρ is constructed by using (2.6).

3. Eigenvalues $\{\lambda_k\}$ and corresponding eigenvectors $\{\boldsymbol{\phi}_k\}$ of $\mathbf{R_x}$ are calculated from (2.17) and (2.20), respectively. Then, eigenvalues are sorted in descending order and corresponding eigenvectors are placed in the eigenmatrix. Thus, $\boldsymbol{\phi}_0$ is the first eigenvector (PC1) and $\boldsymbol{\phi}_1$ is the second one (PC2), and so forth. Eigenvalues of first eleven eigenvectors (principal components) are listed in Table 6.1. These eigenvectors explain 57.2% of the total variance. Due to limited space, only the variable values of SKLT for these eigenvectors are tabulated. Values of $\{\omega_k\}$ that are used to calculate each eigenvalue and corresponding eigenvector also shown in Table 6.1. The root finding algorithm reported in [40] was used.

4. PC loading coefficients (eigenvector components) are fitted to arcsine distribution by calculating $\{a_k = \min(\boldsymbol{\phi}_k)\}\,\forall k$ and $\{b_k = \max(\boldsymbol{\phi}_k)\}\,\forall k$. Then, variances $\left\{\sigma_k^2 = \frac{(b_k - a_k)^2}{8}\right\}\forall k$ are calculated by using (6.7). Table 6.1 also tabulates $\{a_k\}$, $\{b_k\}$ and $\{\sigma_k^2\}$ of eigenvectors.

5. For a given total rate R, $\{R_k\}$ are calculated by plugging $\{\sigma_k^2\}$ in optimum bit allocation equation given in (2.34). Then, quantizer levels $\{L_k\}$ are calculated as $\left\{L_k = 2^{R_k}\right\}\forall k$ and rounded up to the closest odd integer number. R is the sparsity tuning parameter of SKLT. As in all of the sparse PCA methods, R for a given sparsity has to be determined with cross-validation. Table 6.1 displays calculated rates and quantizer levels for the total rate of $R = 5.7$.

6. For this design example, $L = 65$ level pdf-optimized zero-zone quantizer of arcsine distribution with zero mean and unit variance is used as the starting point. Then, several adjacent bins around zero are combined to adjust zero-zone for the desired sparsity level. For k^{th} eigenvector, pre-designed $L = 65$ level pdf-optimized zero-zone quantizer is converted to $L_k \leq L$ level zero-zone quantizer.

7. PC loadings (eigenvector components) are normalized to have zero mean and unit variance, $\left\{\boldsymbol{\phi}_k = \frac{(\boldsymbol{\phi}_k - mean(\boldsymbol{\phi}_k))}{std(\boldsymbol{\phi}_k)}\right\}\forall k$ where *mean* and *std* are the mean and standard deviation of eigenvector components, respectively. Quantized

(sparsed) eigenvectors are generated by applying quantization on eigenvectors of the original eigen subspace $\left\{\widehat{\boldsymbol{\phi}_k} = Q_k\left(\boldsymbol{\phi}_k\right)\right\} \forall k$. Number of zero components or sparsity level $\{S_k\}$ of quantized PCs for this example are also given in Table 6.1.

Number of bins for pre-designed pdf-optimized quantizer is selected based on the quantization noise and implementation cost. The increase in signal-to-quantization noise (SQNR) of pdf-optimized zero-zone quantizer optimized for arcsine pdf with $L > 65$ is found not to be that significant.

Orthogonality Imperfectness and Subspace Sparsity Sparsity achieved by quantization of PCs leads to orthogonality imperfectness. Orthogonality imperfectness ϵ in mse is presented with respect to allowable total rate R (desired sparsity level) for various AR(1) sources as defined

$$\epsilon = \frac{1}{N^2} \sum_{i=0}^{N-1} \sum_{i=0}^{N-1} \left[\mathbf{I}\left(i,j\right) - \mathbf{K}\left(i,j\right)\right]^2 \tag{6.8}$$

where $\mathbf{I}$ is $N \times N$ identity matrix and $\mathbf{K} = \mathbf{A}\mathbf{A}^{*\mathbf{T}}$.

Figure 6.4 displays the trade-off between subspace sparsity and loss of orthogonality for various AR(1) sources and $N = 256$. It is observed from the figure that the orthogonality imperfectness decreases almost linearly with increasing R as expected.

6.3 Sparsity Performance

Now, performance of the proposed SKLT method with the ST [49], SPCA [49], DSPCA [20], and SPC [45] methods is compared for AR(1) process, and also for empirical correlation matrix of stock returns in NASDAQ-100 index in the following subsections. In order to provide a fair comparison, sparsity levels of all methods considered here are tuned in a way that compared PCs have almost same number of non-zero components. In most cases, number of non-zero components of each PC in

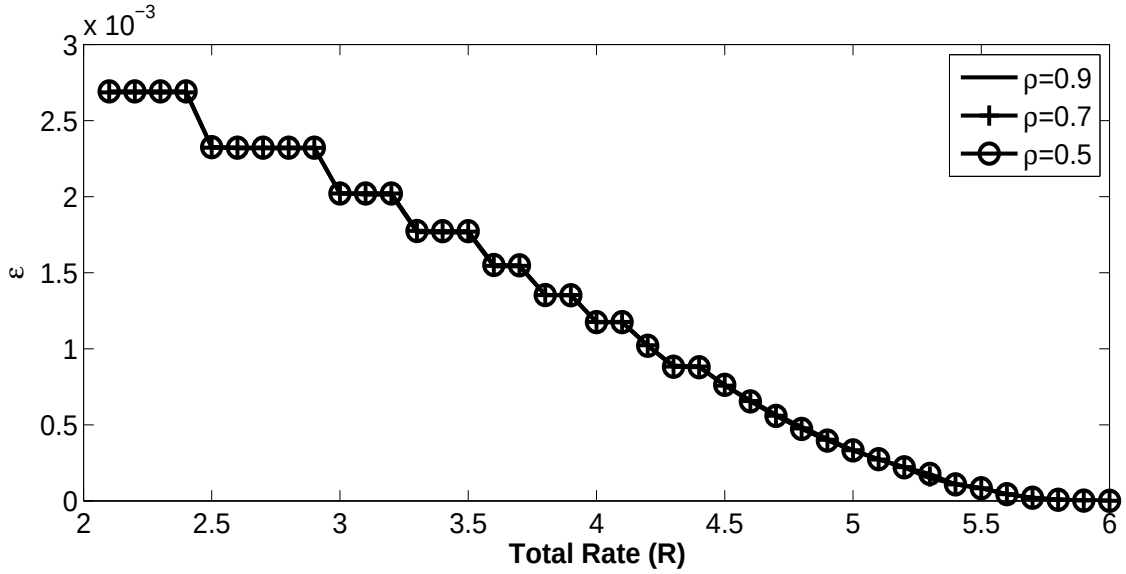

Figure 6.4 Orthogonality imperfectness-rate (sparsity) trade-off of sparse eigen subspaces of three AR(1) sources with $N = 256$.

SKLT method are kept slightly lower than the others in order to show its merit under mildly disadvantageous test conditions.

6.3.1 Sparsity of Eigen Subspace for AR(1) Process

The sparsity imposed on PCs may degrade the explained variance described in [20]. The explained variances (eigenvalues) of the PCs are calculated as

$$\left\{\lambda_k = \sigma_k^2 = \boldsymbol{\phi}_k^{\mathrm{T}} \mathbf{R}_x \boldsymbol{\phi}_k\right\} \forall k \tag{6.9}$$

where $\boldsymbol{\phi}_k$ is the k^{th} eigenvector for a given $\mathbf{R}_x$. For the sparsed PCs, new explained variances (eigenvalue) are calculated as

$$\left\{\widehat{\lambda}_k = \widehat{\sigma_k^2} = \widehat{\boldsymbol{\phi}_k}^{\mathbf{T}} \mathbf{R}_x \widehat{\boldsymbol{\phi}_k}\right\} \forall k \tag{6.10}$$

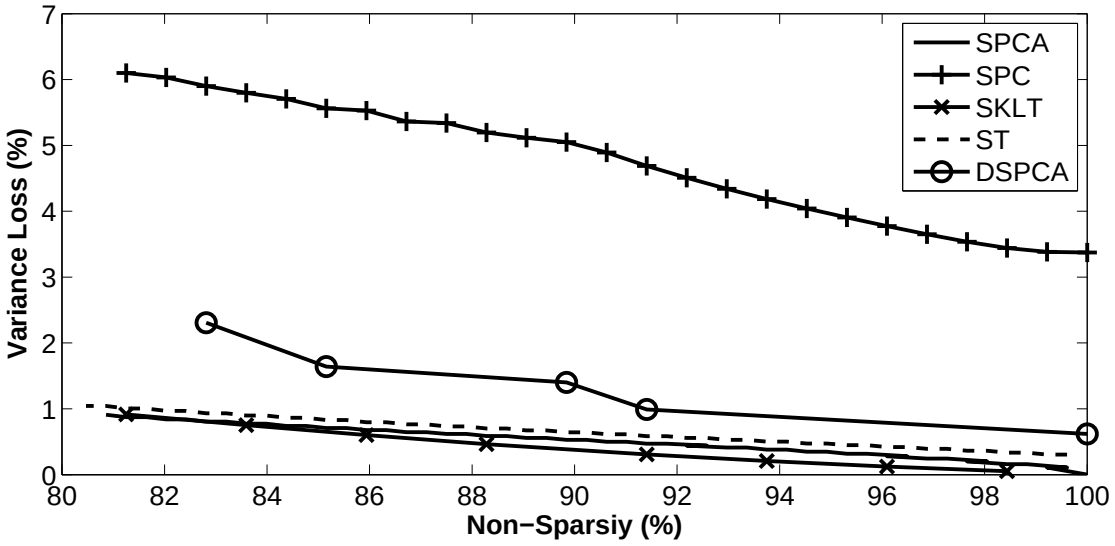

Figure 6.5 Variance loss (VL) measurements of sparsed first PC generated by SKLT, SPCA, SPC, ST and DSPCA methods with respect to non-sparsity (NS) for AR(1) source with $\rho = 0.9$ and $N = 256$.

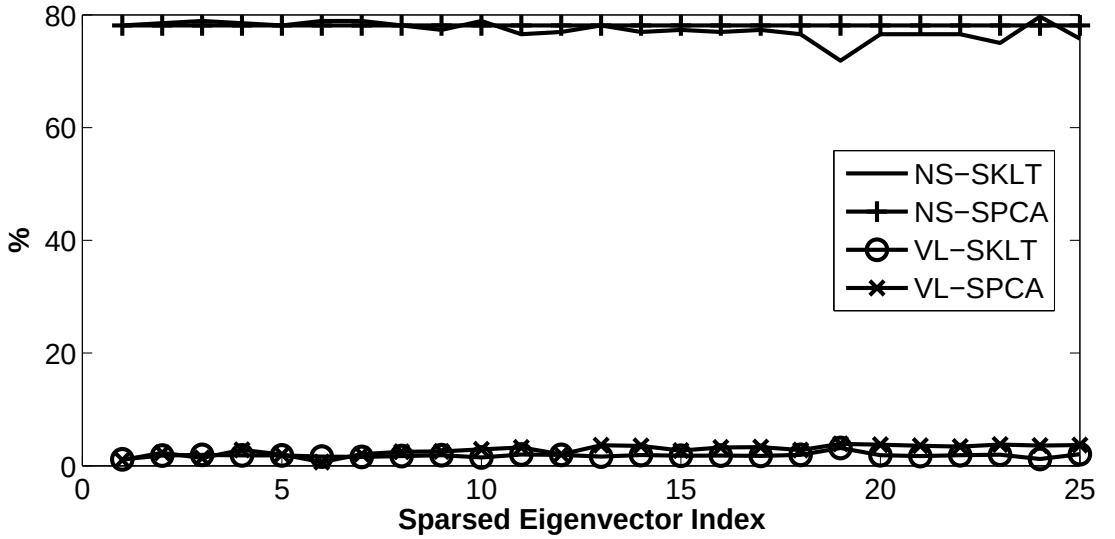

Figure 6.6 Non-sparsity (NS) and variance loss (VL) measurements of sparsed eigenvectors generated by SKLT method and SPCA algorithm for AR(1) source with $\rho = 0.9$ and $N = 256$.

where $\widehat{\boldsymbol{\phi}_k}$ is the k^{th} sparse eigenvector. Then, the percentage of explained variance loss (VL) as a performance metric is defined as

$$\left\{ V_k = \frac{\left(\lambda_k - \widehat{\lambda}_k\right)}{\lambda_k} \times 100 \right\} \forall k \tag{6.11}$$

Cumulative explained variance loss of first L number of PCs is also defined as

$$C_L = \sum_{k=1}^{N} \lambda_k - \sum_{k=1}^{L} \widehat{\lambda}_k \tag{6.12}$$

In addition, non-sparsity (NS) performance metric is also used for comparison. It is defined as the percentage of non-zero components in a given sparsed eigenvector. Thus, the performance is measured as the variance loss for the given non-sparsity level [49, 20, 48]. Their comparative rate-distortion performance cannot be provided due to the lack of models to generate sparse PCs for all methods reported here.

Figure 6.5 displays the variance loss (VL) measurements of sparsed first PC generated by SKLT, SPCA, SPC, ST and DSPCA methods with respect to non-sparsity (NS) for AR(1) source with $\rho = 0.9$ and $N = 256$. For SKLT, $L = 65$ level quantizer optimized for arcsine pdf with zero-mean and unit variance is used as the initial quantizer. The zero-zone width of the initial quantizer is adjusted for required sparsity as explained earlier. Then, the generated quantizer is employed. Figure 6.5 shows that SKLT offers less variance loss than the other methods. SPCA provides competitive performance to SKLT. Figure 6.6 displays non-sparsity (NS) and variance loss (VL) performance comparisons of sparse PCs generated by SKLT and by SPCA for the same AR(1) process. The original eigenvectors that explain 90% of the total variance are selected for sparsity comparison. Figure 6.6 shows that the VL performance of SKLT is slightly better than SPCA. Note that NS of SKLT is slightly lower than SPCA in this comparison.

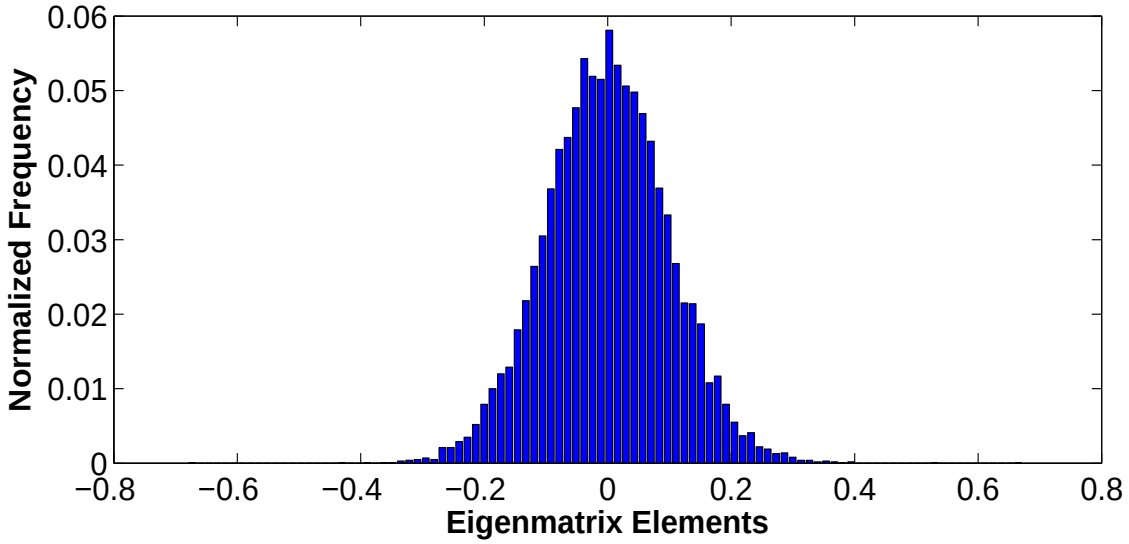

Figure 6.7 Normalized histogram of eigenmatrix elements for empirical correlation matrix of end of day (EOD) returns for 100 stocks in NASDAQ-100 index with $W =$ 30-day measurement window ending on April 9, 2014.

6.3.2 Sparsity of Eigenportfolios for NASDAQ-100 Index

In this section, proposed method is used to sparse eigenportfolios that may lead to trading cost reduction. Empirical correlation matrix for the end of day (EOD) stock returns for NASDAQ-100 index with $W = 30$ day time window ending on April 9, 2014 is measured [41, 2].

The original eigenvectors that explain almost 90% of the total variance are selected for sparsity comparison. Due to simplicity, a single quantizer is employed for the SKLT method to sparse the entire eigenmatrix $\mathbf{A_{KLT}}$. It is optimized for the histogram of its elements as displayed in Figure 6.7. It is observed to be a Gaussian pdf. Figure 6.8 displays the variance loss (VL) measurements of sparsed first PC generated by SKLT, SPCA, SPC, ST and DSPCA methods with respect to non-sparsity (NS). Figure shows that SKLT offers less variance loss than compared methods. Similarly, Figure 6.9 and 6.10 display the cumulative explained variance loss of first sixteen sparsed PCs generated from daily empirical correlation matrix of EOD returns during the time interval between April 9, 2014 and May 22, 2014

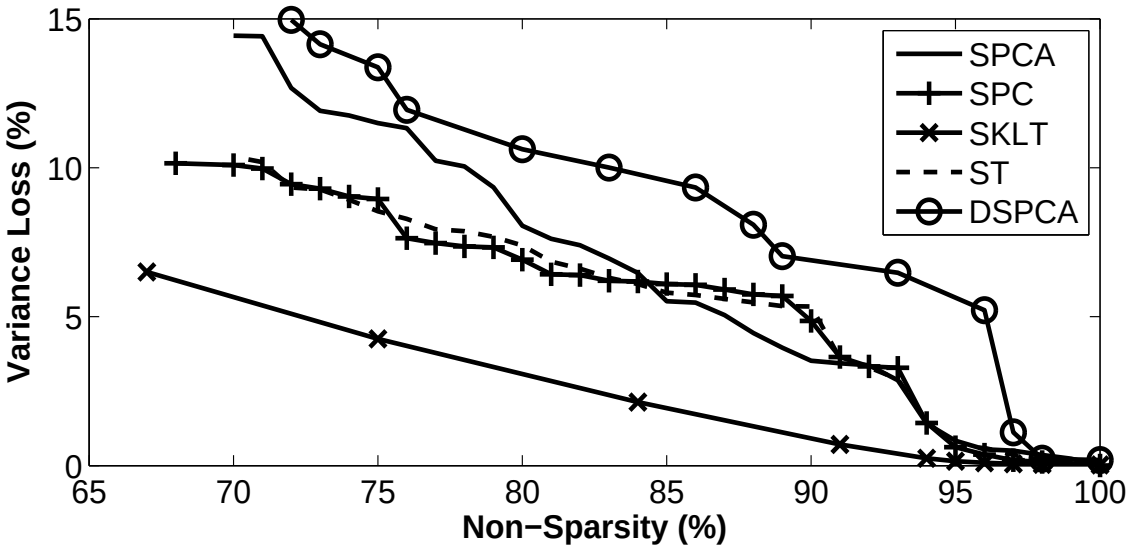

Figure 6.8 Variance loss (VL) measurements of sparsed first PC generated by SKLT, SPCA, SPC, ST and DSPCA methods with respect to non-sparsity (NS) for empirical correlation matrix of end of day (EOD) returns for 100 stocks in NASDAQ-100 index with $W = 30$-day measurement window ending on April 9, 2014.

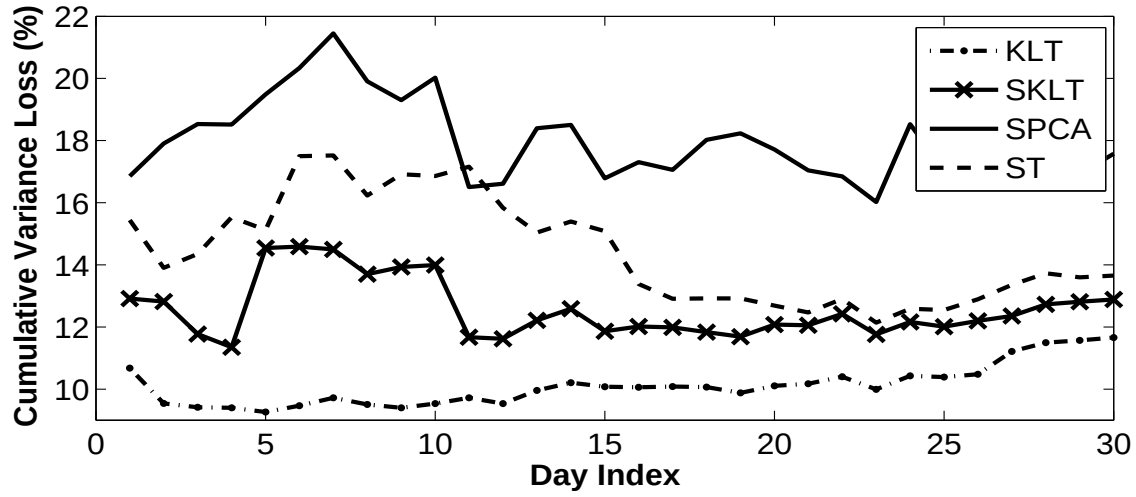

Figure 6.9 Cumulative explained variance loss of first sixteen sparsed PCs generated from daily empirical correlation matrix of EOD returns during the time interval between April 9, 2014 and May 22, 2014 for 100 stocks in NASDAQ-100 index by using KLT, SKLT, SPCA and ST methods. Non-sparsity levels of 85% for each PC is forced with $W = 30$-days.

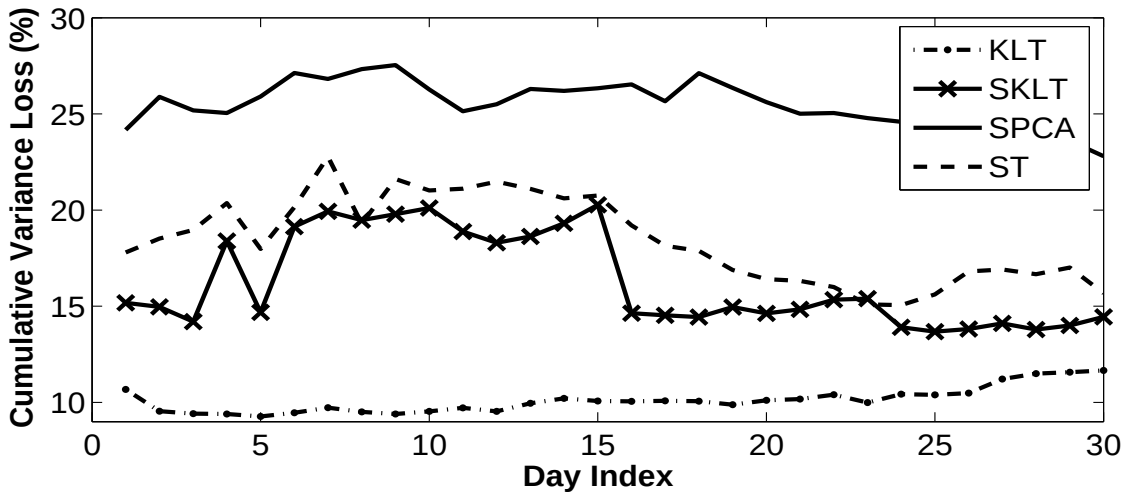

Figure 6.10 Cumulative explained variance loss of first sixteen sparsed PCs generated from daily empirical correlation matrix of EOD returns during the time interval between April 9, 2014 and May 22, 2014 for 100 stocks in NASDAQ-100 index by using KLT, SKLT, SPCA and ST methods. Non-sparsity levels of and 75% for each PC is forced with $W = 30$-days.

for 100 stocks in NASDAQ-100 index by using KLT, SKLT, SPCA and ST methods. The measurement window of the last 30 days, $W = 30$, is used to calculate empirical correlation matrix for each day. Non-sparsity levels of 85% and 75% for each PC are forced in experiments displayed in Figure 6.9 and 6.10, respectively. The superior performance of the SKLT method is observed for this scenario as well where empirical correlation matrix of EOD returns changes every day.

The difference between the original $\mathbf{R}_E(n)$ and the modified correlation matrix $\widehat{\mathbf{R}_E(n)}$ due to sparsed eigenvectors is defined as

$$d^{\mathbf{R}} = \left\| \mathbf{R}_E(n) - \widehat{\mathbf{R}_E(n)} \right\|_2 \tag{6.13}$$

where $\|.\|_2$ is the norm-2 of a matrix. $d^{\mathbf{R}}_{SKLT} = 10.35$, $d^{\mathbf{R}}_{SPCA} = 17.15$, and $d^{\mathbf{R}}_{ST} = 17.38$ are measured for empirical correlation matrix of EOD returns for 100 stocks in NASDAQ-100 index with $W = 30$-days ending on April 9, 2014 with 85% non-sparsity

level. Similarly, the distance between the original and the sparsed eigenmatrices is expressed as

$$d^{\mathbf{A}} = \left\| \mathbf{A}_{KLT} - \widehat{\mathbf{A}_{KLT}} \right\|_2 \tag{6.14}$$

The measured distances for the same experiment are $d^{\mathbf{A}}_{SKLT} = 0.23$, $d^{\mathbf{A}}_{SPCA} = 1.99$, and $d^{\mathbf{A}}_{ST} = 2.00$ for SKLT and ST methods, respectively. These objective measures also show that the proposed SKLT sparses eigen subspace of NASDAQ-100 index better than the ST and SPCA methods for the experiments presented here.

As explained in Chapter 4, the component values of eigenvector $\{\phi_k\}$ are repurposed as the capital allocation coefficients to create the k^{th} eigenportfolio for a group of stocks where the resulting coefficients $\{\theta_k\}$ are pairwise uncorrelated. These coefficients represent eigenportfolio returns in this application. It is required to buy and sell certain stocks in amounts defined by the loading (capital allocation) coefficients in order to build and rebalance eigenportfolios in time. Some of the loading coefficients may have relatively small values where their trading cost becomes a practical concern for portfolio managers. Therefore, sparsing eigen subspace of an empirical correlation matrix $\mathbf{R}_E(n)$ may offer cost reductions in desired portfolio creation, maintenance and trading activity. In contrast, although theoretically appealing, the optimization algorithms like SPCA, DSPCA and SPC with constraints for forced sparsity (cardinality reduction of a set) may substantially alter intrinsic structures of the original eigenportfolios and their assets. Therefore, such a forced sparse representation might cause to significantly deviate from the measured empirical correlation matrix. Hence, financial performance degradations may happen in eigenportfolios generated by sparsity constrained optimization.

6.4 Chapter Summary

The constrained optimization algorithms to generate sparse PCs are unable to guarantee good performance for an arbitrary covariance matrix due to the non-convex nature of the problem. In this paper, we propose a procedure to sparse subspaces. The proposed SKLT method utilizes the mathematical framework developed in rate-distortion theory for transform coding using pdf-optimized quantizers. The sparsity performance comparisons demonstrate the superiority of SKLT over the popular algorithms including ST, SPCA, DSPCA and SPC. SKLT is theoretically tractable, simple to implement and serves to sparse any subspace of interest.

CHAPTER 7

CONCLUSIONS AND FUTURE RESEARCH

In this dissertation, a signal processing framework to design investment portfolios is proposed. Modern Portfolio Theory and subspace methods are investigated and jointly treated. The goal is to understand the behaviour of these subspace methods for finance applications and compare each other for discrete AR(1) signal model. Experiments with real-market data have also been conducted to validate the consistency of the analysis. Moreover, a new method is proposed to sparse a given subspace. It is also compared with the popular methods in the literature.

7.1 Contributions

Contributions of this dissertation are summarized as follows;

1. Eigen and subband subspaces are analytically evaluated and compared using MPT for finance applications. A unified treatment is offered in this dissertation.

2. Closed-form expressions for Sharpe ratio and market exposure of eigenportfolios for discrete AR(1) signal model are derived to evaluate their advantageous and disadvantageous analytically. Performance of eigenportfolios with respect to various model parameters are investigated. The proposed framework presents new insights for trading algorithms like statistical arbitrage that utilize them.

3. Finance application of subband subspace, called subband portfolios, is introduced. Perfect reconstruction filter banks are utilized to generate subband portfolios. Their advantages and disadvantages in terms of Sharpe ratio and market exposure against eigenportfolios are emphasized using the same framework developed to analyze eigenportfolios. It is shown that subband portfolios offer less market exposure with slightly less Sharpe ratio for a given basket.

4. The design of optimized super eigenportfolio (OSEP) is introduced. It is created by optimal allocation of investment capital among eigenportfolios based on maximization of Sharpe ratio. It is shown that OSEP delivers the best Sharpe ratio among eigenportfolios with reasonable market exposure. Same method is applied to generate optimized super subband portfolios (OSSP).

5. A new eigen subspace sparsing method that utilizes the rate-distortion theory is proposed in this dissertation. Its performance is compared with the popular methods in the literature. It is shown that SKLT outperforms those methods for certain cases. The proposed method is also applied to generate sparse eigenportfolios.

7.2 Future Work

1. In the dissertation, discrete AR(1) signal model is used for performance evaluations and comparisons. More sophisticated signal models such as vector auto-regressive, VAR(p), that may give better approximation to financial signals can be used.

2. Although the proposed subspace sparsing method is applicable to any subspace, it is only applied to sparse eigen subspace. Same method should be applied to generate sparse subband subspace. Moreover, the performance evaluations and comparison should be performed for the subband subspace.

BIBLIOGRAPHY

[1] A. N. Akansu and R. A. Haddad. *Multiresolution Signal Decomposition: Transforms, Subbands, and Wavelets.* New York, NY, USA: Academic Press, 1992.

[2] A. N. Akansu and M. U. Torun. *A Primer for Financial Engineering: Financial Signal Processing and Electronic Trading.* New York, NY, USA: Academic Press, 2015.

[3] M. Avellaneda and J. H. Lee. Statistical arbitrage in the US equities market. *Quantitative Finance*, 10(7):761–782, 2010.

[4] M. Bagnoli and T. Bergstrom. Log-concave probability and its applications. *Economic Theory*, 26(2):445–469, Aug. 2005.

[5] N. Balakrishnan and V. B. Nevzorov. *A Primer on Statistical Distributions.* New York, NY, USA: Wiley, 2004.

[6] T. Berger. *Rate-Distortion Theory.* New York, NY, USA: Wiley, 2003.

[7] M. Bertero and P. Boccacci. *Introduction to Inverse Problems in Imaging.* London, UK: Instit. of Physics Publishing, 1998.

[8] N. P. B. Bollen and R. E. Whaley. Hedge fund risk dynamics: Implications for performance appraisal. *The Journal of Finance*, 64(2):985–1035, 2009.

[9] P. Boufounos and R. Baraniuk. Quantization of sparse representations. In *Data Compression Conference, 2007. DCC '07*, pages 378–378, Mar. 2007.

[10] S. Boyd and L. Vandenberghe. *Convex Optimization.* New York, NY, USA: Cambridge University Press, 2004.

[11] J. Brodie, I. Daubechies, C. De Mol, D. Giannone, and I. Loris. Sparse and stable Markowitz portfolios. *Proc. of the National Academy of Sciences*, 106(30):12267–12272, Apr. 2009.

[12] H. Brusewitz. *Quantization with Entropy Constraint and Bounds to the Rate Distortion Function.* Stockholm, Sweden: Telecommunication Theory, Electrical Engineering, Royal Inst. of Technology, 1986.

[13] J. Cadima and I. T. Jolliffe. Loading and correlations in the interpretation of principle components. *Journal of Applied Statistics*, 22(2):203–214, 1995.

[14] H. Caglar, Y. Liu, and A. N. Akansu. Optimal PR-QMF design for subband image coding. *Journal of Visual Communication and Image Representation*, 4(3):242–253, 1993.

[15] H. Caglar, Y. Liu, and A. N. Akansu. Statistically optimized PR-QMF design. In *Visual Communications and Image Processing '91: Visual Communication*, volume 1605, pages 86–94, Nov. 1991.

[16] H. Choi and H. Varian. Predicting the present with Google Trends. *Economic Record*, 88:2–9, 2012.

[17] R. J. Clarke. *Transform Coding of Images.* New York, NY, USA: Academic Press, 1985.

[18] C. A. C. Coello, G. B. Lamont, and D. A. V. Veldhuizen. *Evolutionary Algorithms for Solving Multi-Objective Problems (Genetic and Evolutionary Computation).* Secaucus, NJ, USA: Springer-Verlag New York, Inc., 2006.

[19] S. Darolles, P. Duvaut, and E. Jay. *Multi-factor Models and Signal Processing Techniques: Application to Quantitative Finance.* Hoboken, NJ, USA: Wiley-ISTE, 2013.

[20] A. d'Aspremont, L. El Ghaoui, M. I. Jordan, and G. R. G. Lanckriet. A direct formulation for sparse PCA using semidefinite programming. *SIAM Review*, 49(3):434–448, Jul. 2007.

[21] R. A. Davis. *Gaussian Process, Encyclopedia of Environmetrics.* Hoboken, NJ, USA: John Wiley & Sons, Ltd, 2006.

[22] H. W. Engl, M. Hanke, and A. Neubauer. *Regularization of Inverse Problems.* Dordrecht, Netherlands: Kluwer Academic Publishers, 1996.

[23] C. A. Gonzales and A. N. Akansu. A very efficient low-bit-rate subband image/video codec using shift-only PR-QMF and zero-zone linear quantizers. In *Acoustics, Speech, and Signal Processing, 1997. ICASSP-97., 1997 IEEE International Conference on*, volume 4, pages 2993–2996, Apr. 1997.

[24] A. Hajnal and I. Juhasz. Remarks on the cardinality of compact spaces and their Lindelof subspaces. *Proceedings of the American Mathematical Society*, 51(5):146–148, 1983.

[25] K. Hejn, A. Pacut, and L. Kramarski. The effective resolution measurements in scope of sine-fit test. *Instrumentation and Measurement, IEEE Trans. on*, 47(1):45–50, Feb. 1998.

[26] N. S. Jayant and P. Noll. *Digital Coding of Waveforms: Principles and Applications to Speech and Video.* Englewood Cliffs, NJ, USA: Prentice-Hall Professional Technical Reference, 1984.

[27] K Karhunen. Uber lineare methoden in der wahrscheinlichkeitsrechnung. *Ann. Acad. Sci. Fennicae. Ser. A. I. Math.-Phys.*, 37:1–79, 1947.

[28] A. Leon-Garcia. *Probability, Statistics, and Random Processes for Electrical Engineering.* Upper Saddle River, NJ, USA: Prentice Hall, 2008.

[29] S. Lloyd. Least squares quantization in PCM. *Information Theory, IEEE Trans. on*, Mar. 1982.

[30] M. Loeve. *Probability Theory I.* New York, NY, USA: Springer-Verlag New York, 1977.

[31] H. Mamaysky, M. Spiegel, and H. Zhang. Estimating the dynamics of mutual fund alphas and betas. *Rev. Financ. Stud.*, 21(1):233–264, 2008.

[32] H. M. Markowitz. *Portfolio Selection: Efficient Diversification of Investments.* New York, NY, USA: Wiley, 1959.

[33] J. Max. Quantizing for minimum distortion. *Information Theory, IRE Trans. on*, 6(1):7–12, Mar. 1960.

[34] J. Ohlson and B. Rosenberg. Systematic risk of the CRSP equal-weighted common stock index: A history estimated by stochastic-parameter regression. *The Journal of Business*, 55(1):121–145, Jan. 1982.

[35] K Pearson. On lines and planes of closest fit to systems of points in space. *Philosophical Magazine*, 2(11):559–572, 1901.

[36] W. Ray and R. Driver. Further decomposition of the Karhunen-Loeve series representation of a stationary random process. *Information Theory, IEEE Trans. on*, 16(6):663–668, Sep. 1970.

[37] H. Shen and J. Z. Huang. Sparse principal component analysis via regularized low rank matrix approximation. *J. Multivar. Anal.*, 99(6):1015–1034, Jul. 2008.

[38] R. Tibshirani. Regression shrinkage and selection via the LASSO. *Journal of the Royal Statistical Society, Series B*, 58(1):267–288, 1996.

[39] M. U. Torun and A. N. Akansu. Toeplitz approximation to empirical correlation matrix of asset returns: A signal processing perspective. *Journal of Selected Topics in Signal Processing*, 6(4):319–326, Aug. 2012.

[40] M. U. Torun and A. N. Akansu. An efficient method to derive explicit KLT kernel for first-order autoregressive discrete process. *Signal Processing, IEEE Trans. on*, 61(15):3944–3953, Aug. 2013.

[41] M. U. Torun, A. N. Akansu, and M. Avellaneda. Portfolio risk in multiple frequencies. *IEEE Signal Processing Magazine, Special Issue on Signal Processing for Financial Applications*, 28(5):61–71, Sep. 2011.

[42] N. Trendafilov, I. T. Jolliffe, and M. Uddin. A modified principal component technique based on the LASSO. *Journal of Computational and Graphical Statistics*, 12(3):531–547, Sep. 2003.

[43] R. S. Tsay. *Analysis of Financial Time Series.* Hoboken, NJ, USA: John Wiley & Sons, Inc., 2005.

[44] J. H. Wilkinson. *The Algebraic Eigenvalue Problem.* Oxford, UK: Oxford University Press, 1965.

[45] D. M. Witten, R. Tibshirani, and T. Hastie. A penalized matrix decomposition, with applications to sparse principal components and canonical correlation analysis. *Biostatistics*, 10(3):515–534, Jul. 2009.

[46] V. B. Yee. *Studies on the Asymptotic Behavior of Parameters in Optimal Scalar Quantization.* PhD thesis, The University of Michigan, 2010.

[47] R. Zass and A. Shashua. Nonnegative sparse PCA. In *Neural Information Processing Systems*, pages 1561–1568. MIT Press, 2007.

[48] H. Zou and T. Hastie. Regularization and variable selection via the elastic net. *Journal of the Royal Statistical Society: Series B (Statistical Methodology)*, 67(2):301–320, 2005.

[49] H. Zou, T. Hastie, and R. Tibshirani. Sparse principal component analysis. *Journal of Computational and Graphical Statistics*, 15(2):262–286, 2006.